Hysteresis Patterns of Watershed Nitrogen Retention and Loss over the past 50 years in United States Hydrological Basins

Michelle Newcomer[1], Nicholas J Bouskill[1], Haruko Wainwright[1], Taylor Maavara[2], Bhavna Arora[1], Erica R Siirila-Woodburn[1], Dipankar Dwivedi[1], Ken Williams[1], Carl Steefel[1], and Susan S Hubbard[1]

[1]Lawrence Berkeley National Laboratory
[2]Yale University

November 21, 2022

Abstract

Patterns of watershed nitrogen (N) retention and loss are shaped by how watershed biogeochemical processes retain, biogeochemically transform, and lose incoming atmospheric deposition of N. Loss patterns represented by concentration, discharge, and their associated stream exports are important indicators of watershed N retention patterns because they reveal hysteresis patterns (i.e. return to initial state) or one-way transition patterns (i.e. new steady state) that provide insight into watershed conditions driving long term stream trends. We examined the degree to which Continental U.S. (CONUS) scale deposition patterns (wet and dry atmospheric deposition), vegetation trends, and stream trends can be potential indicators of watershed N-saturation and retention conditions, and how watershed N retention and losses vary over space and time. By synthesizing changes and modalities in watershed nitrogen loss patterns based on stream data from 2200 U.S. watersheds over a 50 year record, our work characterized a new hysteresis conceptual model based on factors driving watershed N-retention and loss, including hydrology, atmospheric inputs, land-use, stream temperature, elevation, and vegetation. Our results show that atmospheric deposition and vegetation productivity groups that have strong positive or negative trends over time are associated with patterns of stream loss that uniquely indicate the stage of watershed N-saturation and reveal unique characteristics of watershed N-retention hysteresis patterns. In particular, regions with increasing atmospheric deposition and increasing vegetation health/biomass patterns have the highest N-retention capacity, become increasingly N-saturated over time, and are associated with the strongest declines in stream N exports—a pattern that is consistent across all land cover categories. In particular, the second largest factor explaining watershed N-retention was in-stream temperature and dissolved organic carbon concentration trends, while land-use explained the least amount of variability in watershed N-retention. Our CONUS scale investigation supports an updated hysteresis conceptual model of watershed N-retention and loss, providing great value to using long-term stream monitoring data as indicators of watershed N hysteresis patterns.

1   **Hysteresis Patterns of Watershed Nitrogen Retention and Loss over**

2   **the past 50 years in United States Hydrological Basins**

3

4   *Michelle E. Newcomer[1], Nicholas J Bouskill[1], Haruko Wainwright[1], Taylor Maavara[2], Bhavna

5   Arora[1], Erica R. Siirila-Woodburn[1], Dipankar Dwivedi[1], Ken Williams[1], Carl Steefel[1], Susan S.

6   Hubbard[1]

7   [1]Lawrence Berkeley National Lab, Earth & Environmental Sciences Area

8   [2]Yale University, School of the Environment

9

10   *Corresponding author: M. Newcomer, mnewcomer@lbl.gov

11

12   **Key Points**:

13   ● Declines in nitrogen (N) exports were documented in 34% of the USGS

14   monitoring stations distributed throughout the CONUS, in areas with increasing N

15   deposition and increasing vegetation health/density patterns

16   ● Watershed N retention undergoing reversal from N saturation displays both

17   unique hysteresis (recovery) patterns and one-way transition patterns to new

18   steady states

19   ● Atmospheric deposition and vegetation productivity/biomass explain up to 45%

20   of the variability in watershed N retention trends

21   ● Land use trends explain the least amount of variability (<10%) of watershed N

22   retention trends

23

24   **Index Terms**: Water quality, Nutrient exports, Watershed Responses

25

26   **Keywords:** Watersheds, Nitrogen dynamics, ecosystem variability, catchment scale nitrogen

27   retention, watershed exports

28

29   **Abstract**

30

31   Patterns of watershed nitrogen (N) retention and loss are shaped by how watershed

32   biogeochemical processes retain, biogeochemically transform, and lose incoming atmospheric

33   deposition of N. Loss patterns represented by concentration, discharge, and their associated

34   stream exports are important indicators of watershed N retention patterns because they reveal

35   hysteresis patterns (i.e. return to initial state) or one-way transition patterns (i.e. new steady state)

36   that provide insight into watershed conditions driving long term stream trends. We examined the

37   degree to which Continental U.S. (CONUS) scale deposition patterns (wet and dry atmospheric

38   deposition), vegetation trends, and stream trends can be potential indicators of watershed N-

39   saturation and retention conditions, and how watershed N retention and losses vary over space

40   and time. By synthesizing changes and modalities in watershed nitrogen loss patterns based on

41   stream data from 2200 U.S. watersheds over a 50 year record, our work characterized a new

42   hysteresis conceptual model based on factors driving watershed N-retention and loss, including

43   hydrology, atmospheric inputs, land-use, stream temperature, elevation, and vegetation. Our

44   results show that atmospheric deposition and vegetation productivity groups that have strong

45   positive or negative trends over time are associated with patterns of stream loss that uniquely

46   indicate the stage of watershed N-saturation and reveal unique characteristics of watershed N-

47 retention hysteresis patterns. In particular, regions with increasing atmospheric deposition and

48 increasing vegetation health/biomass patterns have the highest N-retention capacity, become

49 increasingly N-saturated over time, and are associated with the strongest declines in stream N

50 exports—a pattern that is consistent across all land cover categories. In particular, the second

51 largest factor explaining watershed N-retention was in-stream temperature and dissolved organic

52 carbon concentration trends, while land-use explained the least amount of variability in

53 watershed N-retention. Our CONUS scale investigation supports an updated hysteresis

54 conceptual model of watershed N-retention and loss, providing great value to using long-term

55 stream monitoring data as indicators of watershed N hysteresis patterns.

56

57 **1.0 Introduction**

58   Watershed stream concentrations of nitrogen (N) and carbon (C), and hydrological

59 connectivity driving exports of N and C to coastal zones have been changing around the world.

60 Changes in N and C concentrations and exports (concentration x discharge) are often linked to a

61 variety of direct and indirect causes at watershed scales, many of which examine the degree to

62 which watersheds can retain N (Aber et al., 1998; Bernal et al., 2012; Crawford et al., 2019;

63 Musolff et al., 2016; Smith et al., 1987; Stoddard, 1994; Vuorenmaa et al., 2018). Recent studies

64 indicate that N and C watershed exports have both increased and decreased in watersheds across

65 the continental United States (CONUS) over the last 50 years (Driscoll et al., 2003; Hale et al.,

66 2015; Oelsner et al., 2017; Oelsner & Stets, 2019; Shoda et al., 2019). To explain these trends,

67 studies often point to ecosystems recovering from acidic deposition (Lawrence et al., 2020;

68 Stoddard et al., 1999), recovery from atmospheric N-deposition (Eshleman et al., 2013;

69 Kothawala et al., 2011), watershed management (J. Murphy & Sprague, 2019), and agricultural

70   practices (Renwick et al., 2018; Van Meter & Basu, 2015). Because the watershed

71   biogeochemical characteristics controlling N and C retention, cycling, and loss are a non-linear

72   function of N-deposition, many diverse hypotheses focused on both natural and anthropogenic

73   processes exist to explain trends of in-stream N and C conditions and exports and associated

74   watershed N-retention (Aber et al., 1998; Bernhardt et al., 2005; Guo et al., 2019; Marinos et al.,

75   2018; Stoddard, 1994). Despite the many existing studies examining controls on watershed N

76   retention and loss at regional scales, a comprehensive analysis examining the co-occurrence of

77   watershed N-retention and stream loss patterns has yet to emerge.

78   An important anthropogenic process directly linked to watershed in-stream concentrations of

79   N and C is atmospheric N-deposition. Around the world, atmospheric deposition of N has

80   increased since the industrial revolution (Pinder et al., 2012). Despite air pollution management

81   regulations that have led to declining atmospheric N-deposition trends in some regions (Li et al.,

82   2016), long term N-addition to watersheds has significantly altered the N-retention capacity of

83   watersheds. Specifically, N-retention capacity is the ability to store, retain, or cycle N within the

84   watershed. Retention is balanced by storage and biogeochemical cycling mechanisms that

85   determine release of N which is exported via streams (Stoddard, 1994). N-saturation is a

86   condition whereby N-inputs exceed the biogeochemical retention capacity of the system to

87   release, cycle, store, or retain N within living biomass (plants or microbes) or abiotic ecosystem

88   components (e.g. soils). Once N-saturated conditions are reached, variable rates of C and N

89   release to streams can occur (Pardo et al., 2011). The role of N-deposition on watershed retention

90   of N and release to streams is an ongoing area of research complicated by both terrestrial and

91   aquatic mechanisms.

92   Indeed, much of the debate over whether stream N is a function of atmospheric N deposition

93   is centered on the degree to which watersheds can either retain and release N through biotic and

94   abiotic factors (Aber et al., 2003; Lovett et al., 2000; Stoddard, 1994). Foundational nitrogen

95   studies have hypothesized that alleviation of nitrogen limitation in soils have led to increased

96   nitrate mobility, positive effects on vegetation productivity (Aber et al., 1998), and subsequent

97   mobilization of nitrogen to streams (Stoddard, 1994). Once inputs surpass biological demand, the

98   watershed may become N-saturated, and additional supply may lead to vegetation mortality

99   through decreased cation availability (Lucas et al., 2011; Shultz et al., 2018), enhancing N

100   transport through nitrification and mineralization. Observations of decadal declines in N

101   concentrations and exports in streams despite increased N-deposition have confounded many of

102   these foundational ideas (Goodale et al., 2003; Lucas et al., 2016). More recently however,

103   significant reductions atmospheric N deposition in some regions have reinvigorated research

104   around this topic because of the opportunity afforded by this natural experiment to test these

105   hypotheses (Eshleman et al., 2013).

106   Observations of trends in watershed N and C exports and concentration in streams have been

107   proposed as potential indicators of watershed N-retention status because stream exports relate to

108   landscape release patterns as indirect measurements of those same processes (Goodale et al.,

109   2005). An extensive body of research has examined such stream measurements at regional-

110   scales. Multi-decadal trends in surface water solute chemistry and exports of dissolved organic

111   carbon (DOC) and dissolved inorganic nitrogen (DIN) have been identified as a function of

112   watershed characteristics, climate, and anthropogenic factors (Ballard et al., 2019; Bellmore et

113   al., 2018; Boyer et al., 2006; Moatar et al., 2017; Musolff et al., 2015; Oelsner & Stets, 2019;

114   Shoda et al., 2019; Stoddard et al., 1999; Zarnetske et al., 2018). Many studies have examined

115   the role of atmospheric N-deposition (Driscoll et al., 2003; Monteith et al., 2007; Musolff et al.,

116   2017; Stoddard et al., 1999, 2016). The role of changing atmospheric loading on watershed N

117   retention is confounded by other hydrobiogeochemical and landscape variables including

118   geology, vegetation, soil characteristics, microbial communities, land cover/land use, climate,

119   wetland cover (e.g. (Aber et al., 2003; Bellmore et al., 2018; Boyer et al., 2006; Stoddard, 1994))

120   as well as disturbances, such as wildfire (Jensen et al., 2017; S. F. Murphy et al., 2015; Rhoades

121   et al., 2018). Because atmospherically deposited N is involved in range of biotic and abiotic

122   transformations and redox cycling before reaching the stream, stream DIN and DOC exports may

123   either deviate from or mirror atmospheric deposition trends (Argerich et al., 2013; Bernal et al.,

124   2012; Halliday et al., 2013; Lovett et al., 2000; Musolff et al., 2015; SanClements et al., 2018).

125   A suite of mechanistic biogeochemical controls in the landscape have been identified as

126   factors relating watershed N-retention to stream exports. Addition of N on the landscape has

127   been documented to impact the following mechanisms: soil microbial

128   mineralization/immobilization, and abiotic immobilization (Goodale et al., 2005; Huntington,

129   2005; Lovett et al., 2018), biotic uptake (Goodale et al., 2005; Huntington, 2005; Yanai et al.,

130   2013), declining organic matter decomposition (Bowden et al., 2019; Janssens et al., 2010),

131   shifting soil C:N ratios (Groffman et al., 2018; Yanai et al., 2013) leading to specific

132   thresholding behavior for N release to streams (Evans et al., 2006), and altered soil organic

133   carbon composition (Bowden et al., 2019; Evans et al., 2006) including declines in the rapidly

134   cycling labile carbon pools (Cusack et al., 2011). In addition, complex internal soil mechanisms

135   responding to increasing atmospheric CO_2 have been found to drive increased N retention and

136   soil carbon cycling limiting stocks of labile organic carbon (Groffman et al., 2018; Hungate et

137   al., 1997; Huntington, 2005).

138   Once N and C reach the stream, additional biogeochemical mechanisms exist that impact

139   stream exports. In-stream response to variable DOC lability (Groffman et al., 2018; O'Donnell et

140   al., 2010) can impact in-stream and hyporheic denitrification (Goodale et al., 2005) tilting

141   streams towards thermodynamic limitations (e.g. monomeric and polymeric carbon) rather than

142   kinetic limitations (e.g. concentration) (Garayburu-Caruso et al., 2020; Stegen et al., 2018). The

143   pool of C and N that reaches the stream is also determined by hydrological conditions that shift

144   stream water from fast to slow flow paths (i.e. runoff and infiltration partitioning). Deeper flows

145   can access more aged, microbially sourced carbon pools (nonaromatic, recalcitrant), while more

146   shallow flows access more young terrestrially derived carbon from vegetation and soils (Barnes

147   et al., 2018). Given that shifts in precipitation are expected to be the dominant driver of changes

148   in partitioning of runoff and infiltration as primary sources of water to streams (difference

149   between young versus older water), as well as evapotranspiration drivers of water table

150   fluctuations, changes in hydrology are quite likely to affect flow paths and access to different

151   sources of carbon of varying characteristics. Regionally, even slightly dryer conditions or greater

152   evapotranspiration can lead to deeper flow paths and longer residence times providing access to

153   legacy nitrogen sources which would increase watershed exports despite little to no change in

154   discharge. Legacy nitrogen is a potentially confounding variable that may impact direct analysis

155   of watershed retention (Van Meter et al., 2016; Van Meter & Basu, 2015).

156   Despite these complexities discussed above, conceptual models examining connections

157   between soil, atmospheric, vegetation, and stream water trends as indicators of and responses to

158   deposition conditions have significantly advanced understanding of watershed response to

159   decadal atmospheric N addition. Such conceptual models have identified many trajectories for

160   landscape evolution after decades of atmospheric N deposition—watersheds may either return to

161   the initial state after the perturbation (hysteresis), or transition to a new stable state (one-way

162   transition) (Aber et al., 1998; Lovett et al., 2018; Vitousek & Reiners, 1975). Hysteresis in this

163   sense refers to the recovery of the watershed to the original state, but through a different path.

164   More recent conceptual models include previously unrecognized mechanisms related to soil N

165   re-accumulation and storage (Lovett et al., 2018; Lovett & Goodale, 2011) and loss of base

166   cations within soil (Lawrence et al., 2020). Observations of decadal long stream N and C

167   hysteresis patterns, driven in some cases by state shifts between interacting soil mycorrhizal,

168   microbial and plant communities after N deposition declines, point to the potential for biotic and

169   abiotic conditions within watersheds to either reach a new equilibrium state or display hysteresis

170   under declining N-deposition (i.e. recovery) (Gilliam et al., 2019). While these recent studies

171   have advanced new conceptual models at the regional scale, they have yet to be tested against

172   CONUS scale trends relative to watershed inputs and outputs. New insights and conceptual

173   models will be needed to frame these stream trends in the context of important watershed

174   characteristics and the vast amount of aquatic and terrestrial data available (Figure 1).

175

$$\frac{dI}{dt} - \frac{dV}{dt} - \frac{dS}{dt} - \frac{dG}{dt} = \frac{dE}{dt}$$
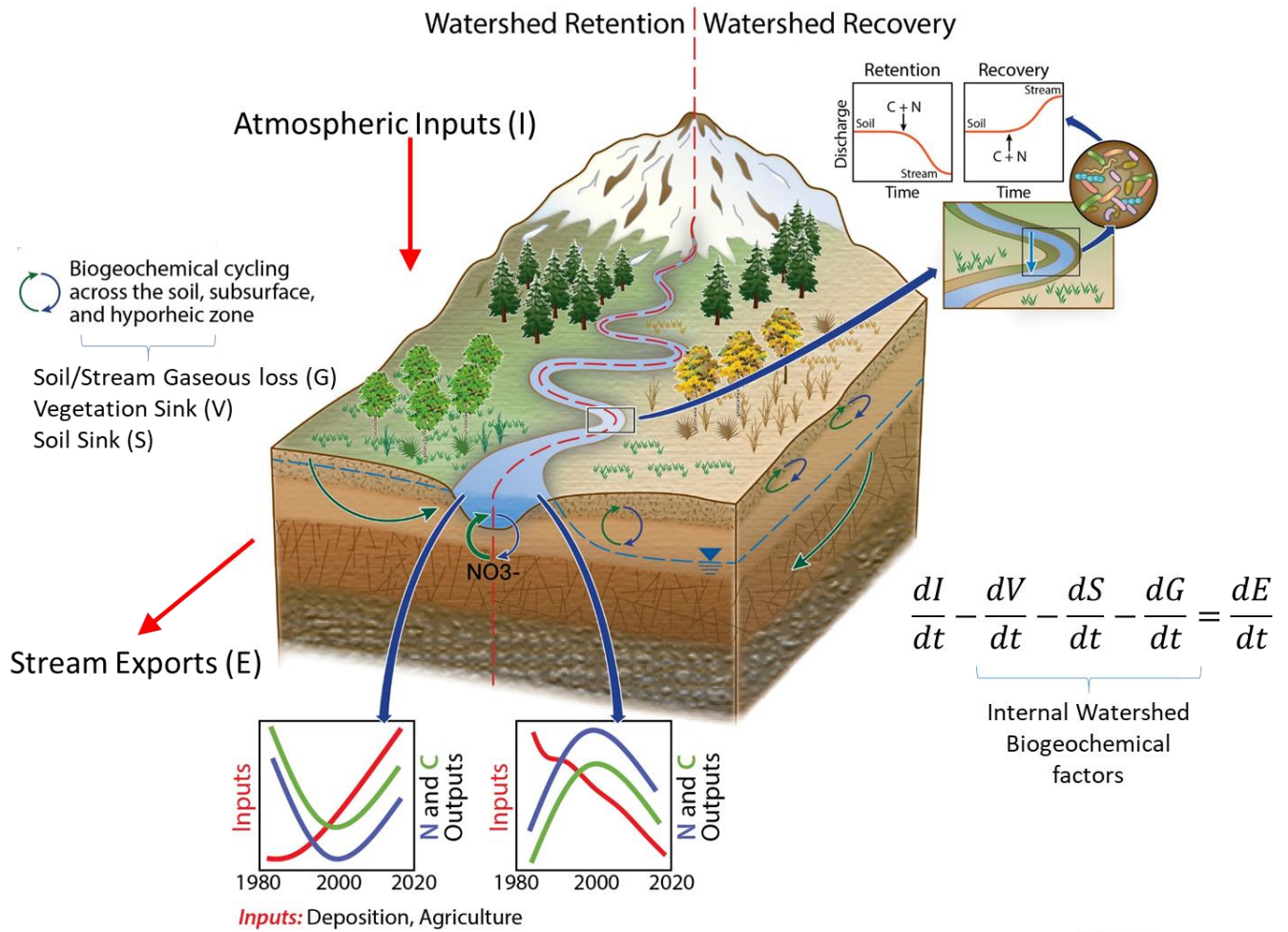
176

177 Figure 1: Hydro-biogeochemical processes occurring from bedrock to canopy and across

178 elevation gradients influence the retention and transformation of input atmospheric N deposition

179 (I), leading to distinct export signatures (E). During the progressive stages of atmospheric

180 deposition of N, watersheds have the capacity to retain N through various soil and vegetation

181 sink terms, and biogeochemical processes leading to reduced C and N delivery to streams, and

182 export patterns unique to the 'watershed retention' stage (left side of watershed). During the

183 recessive stage of atmospheric deposition, 'watershed recovery' occurs from decreased

184 atmospheric deposition loadings, and watersheds exhibit unique patterns of stream export in

185 response to greater movement of C and N from soils to stream (right side of watershed). The

186   watershed equation is modified from Lovett & Goodale (2011) where *dI/dt* is the Input rate,

187   *dV/dt* is the rate of vegetation uptake, *dS/dt* is the soil sink rate, dG/dt is the soil and stream

188   gaseous loss rate, and *dE/dt* is the stream export rate. Inputs, vegetation, and exports were all

189   evaluated at the yearly and seasonal time scales.

190

191   In the present study, we examine the degree to which CONUS scale atmospheric deposition

192   patterns, vegetation trends, and stream trends can potentially be indicators of watershed N-

193   saturation, retention, and recovery conditions. We also examine how watershed N retention and

194   losses vary over space and time. In this work we define watershed N losses as the stream export

195   term, atmospheric deposition as the input term, and the difference between inputs and losses

196   being equal to the internal soil, vegetative, and gaseous biogeochemical cycling terms (i.e. soil

197   and aquatic denitrification) (Eshleman et al., 2013). We do not directly analyze internal

198   biogeochemical cycling terms in this study (i.e. soil and aquatic denitrification, gaseous loss), but

199   we use knowledge of these mechanisms from many prior studies to help develop our conceptual

200   model. Our four stage hysteresis conceptual model of N-saturation and associated stream exports

201   allows for reversal and recovery (i.e. hysteresis) or complete transition to a new stable steady

202   state following the combined factors including atmospheric deposition trends, vegetation trends

203   represented by remote-sensing measurements of NDVI, and stream conditions to explain trends

204   (Lovett et al., 2000). With a reversal of N-deposition reported, we hypothesize this conceptual

205   model will account for the wide variety of observed N concentration and export trends.

206   The four groups that are hypothesized to contribute to N and C export as a function of

207   atmospheric N-deposition and vegetation NDVI trends are depicted in Figure 2:

10

208   ● Group a, Retention: Retention capacity is at its highest (can retain most of incoming N

209   deposition). Watershed retention of incoming N deposition is close to 100% indicated by

210   small watershed exports relative to deposition. This group is represented by locations

211   where total atmospheric N deposition and vegetation health/biomass indices (represented

212   by Normalized Difference Vegetation Index, NDVI) are increasing, leading to elevated N

213   retention. Stream exports of N and C decline due to net immobilization in soils, high

214   stream denitrification and biological uptake from more thermodynamically favorable

215   (more labile) carbon delivered to the stream and produced in the stream from

216   photoautotrophs. These watersheds have not yet reached N-saturation loosely quantified

217   by soil C/N molar ratios that are > 40 (Evans et al., 2006).

218   ● Group b, Saturation: Retention capacity is still at its highest but approaching saturated

219   conditions. Watershed retention of incoming N deposition is close to 100% indicated by

220   small watershed exports relative to deposition, and some watersheds may indicate

221   saturated conditions by showing declines in retention through increasing export trends.

222   This group is represented by locations where total N-deposition continues to increase

223   over time, but vegetation biomass/productivity indices decline (negative NDVI trends).

224   These watersheds generally show soil C/N ratios that are < 40. While N immobilization

225   slows as biotic and abiotic stores become saturated, C and N delivery to streams is

226   limited because landscape retention is still occurring. Moreover, continued stream

227   denitrification leads to a lack of any obvious saturation or trend signal in water quality,

228   accompanied by observations of predominant decreasing trends of riverine nitrogen,

229   albeit with some increasing trends in DIN and labile DOC.

230   ●   Group c, Release: As watersheds undergo regional declines in atmospheric N deposition

231   after experiencing periods of elevated atmospheric N deposition, vegetation

232   biomass/productivity indices improve (positive NDVI trends), soils remain saturated in N

233   relative to C, and N release from soils to streams continues. Even though leaching of N

234   and organic matter to streams increases due to saturated conditions, immobilization and

235   deeper N storage within soil horizons may continue but at a greatly declining rate

236   depending on soil biotic/abiotic/microbial processes. Carbon begins to shift to a less

237   thermodynamically favorable state (less labile) thereby limiting in-stream microbial

238   denitrification, leading an increase in C export. In some locations it would be expected

239   that stream exports of N increase because of the reduced capacity for soil N storage and

240   from limited denitrification.

241   ●   Group d, Recovery: In the final stage of reversal from N-deposition, vegetation health

242   indices show some signs of decline because of a return to N limiting conditions, soil

243   provisions of N and C to the stream begin to increase as soil immobilization plateaus and

244   C/N ratios rise above 40. Even though soil C and N delivery to streams continues,

245   continued decline of thermodynamically favorable carbon to streams limits denitrification

246   potential and allows for continuous increases in stream exports of N.
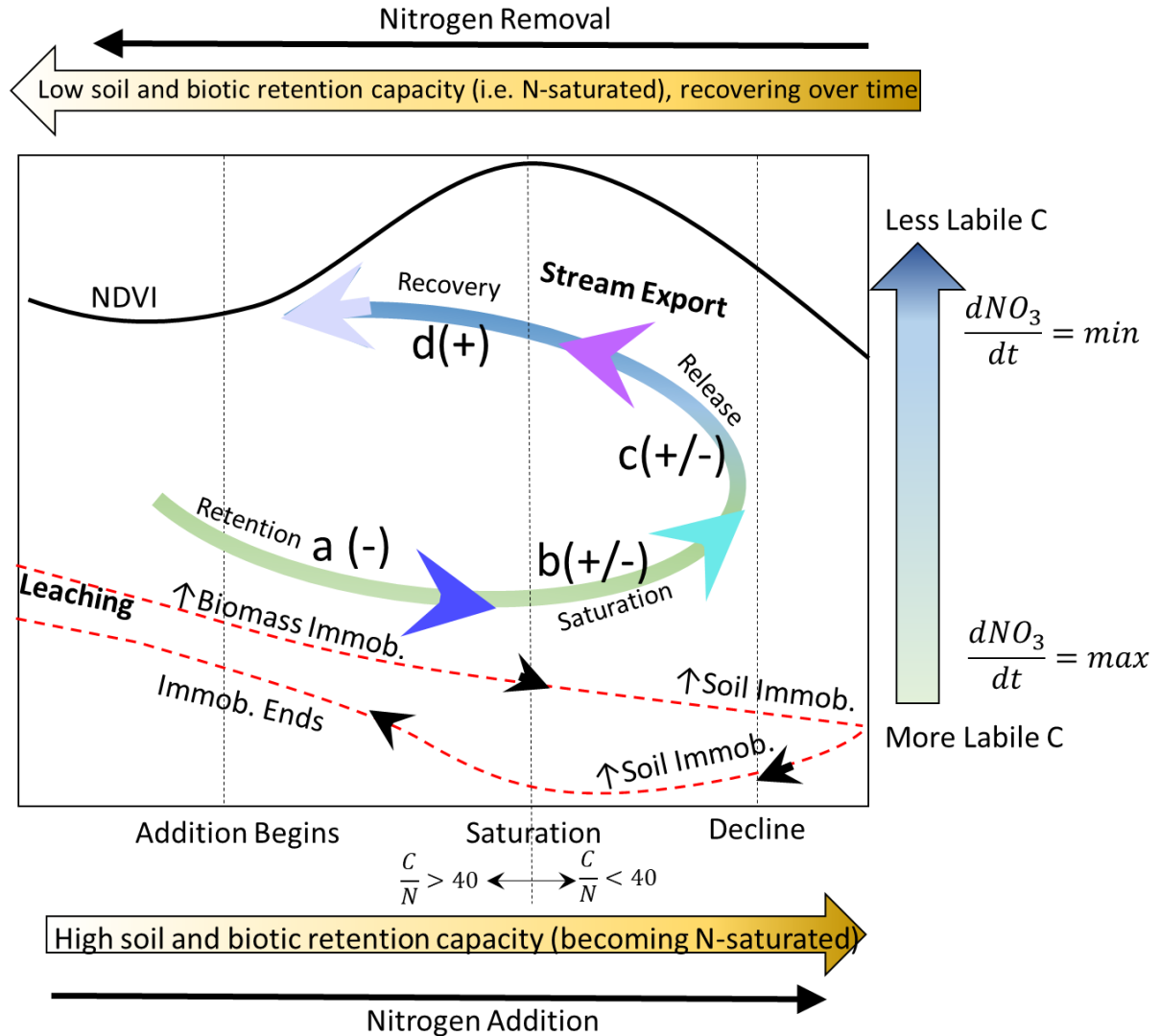
247

248

Figure 2: Our updated conceptual model of responses to N-saturation within watersheds showing

the hysteresis pattern of N exports moving from retention to recovery. Figure modified from

concepts described by Aber and Stoddard in prior studies (Aber et al., 1998; Stoddard, 1994) and

others (Gilliam et al., 2019). The groupings a, b, c, and d, represent different stages on the

hypothesized hysteresis curve of vegetation and NO_3 delivery response to N-deposition

referenced in-text below. Group a should show a decline in stream exports (as indicated by '-'),

Groups b and c show variable (+/-) stream exports depending on the other conditions, and Group

d should show increases (+) in stream exports. Leaching, the process of soil delivery of N and C

257   to streams is shown by the red dashed line and is represented as a function of soil and biomass

258   immobilization. While immobilization occurs, leaching is reduced until immobilization ends.

259

260   Using the conceptual model outlining N-dynamics illustrated in Figure 2, our goal is to

261   identify and quantify watershed N retention conditions, hysteresis patterns, and transitions across

262   the CONUS using stream concentration and export indicators. The knowledge gaps related to

263   watershed N-retention highlighted above motivate three research questions that we address: 1)

264   How are in-stream N and C concentrations (Cn) and exports *(Ex)* changing, both annually and

265   seasonally, and how do these changes relate to discharge (Qs), vegetation, land-use, and

266   atmospheric N deposition? 2) Do stream water quality trends support the hypothesized groups of

267   watershed N-retention and provide evidence for hysteresis patterns? 3) Can groups of changing

268   TDEP and NDVI provide insight into hydro-biogeochemical processes controlling watershed

269   export trends and watershed N-retention hysteresis or one-way transition patterns? We conduct

270   this work over the CONUS scale to quantify and track where retention patterns are changing, and

271   to provide conceptual guidance for large scale controlling factors on these trends including the

272   role of deposition, vegetation, land-use, and in-stream conditions.

273   To evaluate how watersheds across the US have responded to changes in depositional trends,

274   we calculate decadal trends in stream concentrations and exports of C and N such as dissolved

275   inorganic nitrogen (DIN) and dissolved organic carbon (DOC). We examine five variables of

276   interest that are available at the CONUS scale and that represent controls on in-stream DIN

277   concentrations and exports: net (wet+dry) atmospheric N-deposition, land-use and change,

278   elevation, NDVI, and stream characteristics (temperature and DOC trends). We calculate trends

279   using yearly and seasonal statistics across the last half-century of data acquired by the USGS and

280   aggregate station trends using station and Hydrological Unit Code (HUC) scales across the

281   CONUS. Statistics include trends in-stream concentrations (*Cn*), temperatures (*T*), discharge

282   rates and volumes (*Qs*), bulk surface water mass exports (*Ex*), and bulk surface water area

283   normalized mass exports or yields (*Ys*). We use the HUC scales as the watershed aggregating

284   units.

285

286   **2.0 Materials and Methods**

287   We analyzed in-stream C and N concentrations and discharge from USGS National Water

288   Information System (NWIS) stations across the U.S. of six different nitrogen parameters

289   (Supplementary Table A1), one carbon parameter, and temperature (USGS, 2016, 2018)

290   (https://waterdata.usgs.gov/nwis). This big-data approach requires automated analysis to retrieve

291   U.S. Geological streamflow, and concentration data from the long-term monitoring network

292   NWIS using available USGS Web services (Read et al., 2017). We calculated a time-series of

293   total mass exports past a stream station *Ex(t)* (kg/year) using the discharge *Qs(t)* and

294   concentration *Cn(t)* time series by integrating from day 1 of each water year to day 365 for

295   annual time series, and every 3 months for seasonal exports (Equation 1). The mass export is the

296   multiplication of discharge *Qs(t)* (m^3/day) and concentration *Cn(t)* (mg/L converted to kg/m^3)

297   and summed for all daily time steps (dt). Yields were calculated by dividing the total mass export

298   *Ex(t)* (Kg/year or Mg/year) by the drainage area (DA, km^2 or hectare) contributing to watershed

299   yield at that particular station (Kg/km^2/year or Mg/km^2/year) (Equation 2). We converted all

300   values to Kg/hectare, which is the unit associated with the atmospheric deposition time-series.

301

302   (1) Export=$Ex(t)$= $\sum_{day\ 1}^{day\ 365} Qs(t)Cn(t)dt$

303

304 (2) Yield=$Ys(T)$=$\dfrac{\sum_{day\,1}^{day\,365} Qs(t)Cn(t)dt}{DA} = \dfrac{Export}{DA}$

305

306   Initial NWIS station selection was based on the criteria that a station was 'maintained' over

307 time and not sampled just once. If a station had *any* available data for *Cn* and *Qs* defined as at

308 least 20 observations of *any* measurements, the station was selected for the next step (see

309 Supplementary Figures A1-A7 for data downloading methods and for station text files). We then

310 subset stations with the criteria that available *Cn* data span across a minimum of 15 years, and

311 contained at least 50 measurements of that *particular* parameter with associated daily *Qs* data.

312 We required stations to have both *Qs* and *Cn* data available (see Supplementary Information A

313 for methods and station files for each NWIS parameter). Since not all NWIS parameters are

314 available at all stations, we used a different set of stations for each parameter. All NWIS data is

315 retrievable through the R packages EGRET and dataRetrieval (Hirsch & De Cicco, 2015).

316 Exports and Yields were calculated at the yearly and seasonal time-scale with daily *Qs-Cn* values

317 requiring 365 data points for yearly calculations, and 90 for seasonal calculations. When *Cn* was

318 not available for a particular day, we used a gap-filling approach described below (section 2.1).

319   The final selection criteria considers the completeness of the station's data across the

320 different hydrologic unit code (HUC) 2-8 scales, and their distribution across elevation

321 categories (Table 1). Each hydrologic unit is identified by a unique HUC consisting of two to

322 eight digits based on the four levels of classification in the hydrologic unit system. As defined by

323 the U.S. Geological Survey, HUC 2-8 scales divide the U.S. into successively smaller hydrologic

324 units which are classified into four levels: regions, sub-regions, accounting units, and cataloging

325 units represented in more common terminology as basin to sub-watershed scales (Seaber et al.,

326   1987). HUC2 scales represent the largest hydrological region (basin-scales) while HUC8 scales

327   are nested within HUC2 scales and represent cataloging units often referred to as sub-

328   catchments. HUC2 scales represent the largest basin unit within the U.S that contains nested

329   smaller watersheds (Supplementary Table A2 and Supplementary Figure A1). There are 22

330   distinct HUC2 basins within the U.S that are the largest representative basins (Supplementary

331   Table A2).

332

333   Table 1: Information about the number of stations across elevation categories for each NWIS

334   parameter, the range of time water quality data were collected, and the statistics of watershed

335   completeness (i.e. the percentage of watersheds that the stations are found in relative to the total

336   number of watersheds in a given HUC).

			Elevation Categories (m)					Watershed Completeness			
Parameter ID	Short Name	Number of Stations	0-100	100-1000	1000-3000	3000-5000	Time-Series Range	HUC2 (n=22)	HUC4 (n=280)	HUC6 (n=440)	HUC8 (n=2200)
00630	TIN	4988	228	500	896	301	1901-2019*	100.0%	76.1%	78.6%	58.3%
00631	DIN	5666	223	509	937	419	1901-2019	100.0%	77.9%	80.2%	63.2%
00600	TN	6046	260	548	986	378	1901-2019	100.0%	76.4%	80.0%	62.0%
00602	TDN	2650	164	320	492	203	1959-2019	100.0%	75.4%	77.5%	44.4%
00608	DAA	4790	213	443	921	361	1901-2019	100.0%	75.0%	77.0%	58.6%
00610	TAA	5366	238	511	882	297	1901-2019	100.0%	76.1%	78.6%	57.3%
00681	DOC	2520	156	272	443	160	1959-2019	100.0%	76.1%	77.3%	44.2%
00010	Temp	1906	101	175	456	202	1951-2019	95.5%	66.4%	62.3%	36.6%

Descriptions from: https://www.waterqualitydata.us/public_srsnames/

*NWISID 09364500 for ANIMAS RIVER AT FARMINGTON, NM is the station with the longest time series. First collected sample was in September 1900 and no collected occurred thereafter until 1971 representing a 70 year gap.

337

338

339   **2.1 Gap-filling Datasets**

340   To overcome the problem of sparse concentration and daily discharge data, discharge $Qs(t)$

341   and concentration $Cn(t)$ time-series statistics are used to gap-fill the Cn time-series using the

342   USGS Weighted Regressions based on Trends, Discharge, and Seasonality (WRTDS) method

343   (Hirsch et al., 2010; Hirsch & De Cicco, 2015; Sinha & Michalak, 2016; Van Meter & Basu,

344   2017). Additionally, the averaging method (Kothawala et al., 2011; Lovett et al., 2000; Quilbé et

345   al., 2006), and last-observation carried forward (LOCF) method (Moritz et al., 2015) were

346   implemented for comparison to the WRTDS method, the detailed analysis and results of which

347   are found in the Supplementary Information B-Additional Results. Gap-filling methods are

348   necessary for the $Cn(t)$ time-series because Equation 1 cannot be calculated for yearly or

349   seasonal exports if Cn is not available at each daily time-step. An advantage of WRTDS is the

350   prediction of Cn based on Qs-Cn statistical relationships to obtain hind-cast Cn estimates when

351   Qs is available. The main drawback of WRTDS is that the hind-casting of Cn based on historical

352   Qs is often difficult to predict when dry years follow wet years (Pellerin et al., 2014). The R

353   package EGRET offers two predictions of Cn: the mean Cn based on measured Qs and the

354   statistical Qs-Cn relationship, and the flow normalized Cn (FNC) which is a normalized value

355   calculated based on the probability density function of Qs during that given day assuming that

356   the distribution of discharge is stationary (see EGRET user manual for additional information

357   (Hirsch & De Cicco, 2015)). The FNC removes the random variability in Cn driven by the

358   random variability in Qs. EGRET also offers two predictions of export Ex: the Ex based on the

359   mean Cn and measured Qs, and the flow normalized Ex (FNE) which is a normalized export

360   value calculation based on the FNC prediction given the probability density function of Qs.

361

362   **2.2 Trend Detection and Statistical Significance**

18

363   We analyzed concentration time-series *Cn(t)*, flow normalized concentration time-series

364   *FNC(t)*, export time-series *Ex(t)*, flow normalized export time series *FNE(t)*, yield time series

365   *Y(t),* flow normalized yield time series *FNY(t),* and discharge time-series *Qs(t)*. We calculated

366   trends for each nitrogen (N) and carbon (C) parameter using two techniques: 1) linear models to

367   extract the slope (β) representing the trend, and 2) Mann-Kendall tests to extract the slope (β$_{MK}$)

368   representing the trend (Forbes et al., 2019; Helsel & Hirsch, 2002). We analyzed a suite of

369   statistics using the R statistical software for each time series including yearly and seasonal

370   minimum, maximum, and mean values and trends (R Core Team, 2014). Linear models and

371   Mann-Kendall trend tests were only constructed for stations that had >15 years of data available

372   after gap-filling with WRTDS. The predictions and calculations for concentration time-series

373   *Cn(t)* are shown (Equation 3) with concentration (*Cn*) mg/L, slope (β) mg/L/year, time (t) year,

374   and intercept (I) mg/L.

375

376   (3) Linear model $Cn(t) = \beta t + I$

377

378   Statistical significance of trend tests and persistence of trends were obtained from 1) the

379   significance p-value for the linear slope β at the $p<0.05$ value, 2) the significance p-value for the

380   Mann-Kendall trend parameter β$_{MK}$ (Helsel & Hirsch, 2002) at the $p<0.05$ value, and 3) by

381   calculating the persistence of trends using the Hurst Persistence analysis technique (Dwivedi &

382   Mohanty, 2016; Hurst, 1951) using Hs=0.6 as the persistence cutoff value. We looked at

383   statistical significance of trends using the three methods outlined above to provide robustness to

384   the interpretation of trends (Renwick et al., 2018; Wasserstein & Lazar, 2016).

385

386   **2.3 Net Atmospheric Deposition, Elevation, Land Cover, and Normalized**

387   **Differenced Vegetation Index**

388   We directly compared trends in six environmental variables of interest—atmospheric wet and

389   dry N-deposition, land-use/land-use change, stream conditions (temperature and DOC),

390   elevation, drainage area, and Normalized Differenced Vegetation Index (NDVI)—to trends in

391   surface water quality exports and yields. We analyzed the total wet and dry deposition (TDEP,

392   Kg/hectare) of all nitrogen species including NO_3^- and NH_4^+ at the yearly time scale across

393   CONUS from a composite TDEP product available as a smoothed, yearly (once per year) gap-

394   filled CONUS product for years 2000-2018 (NADP, 2018; Schwede & Lear, 2014). The TDEP

395   wet and dry product is a composite product that utilizes the wet deposition product from the

396   National Atmospheric Deposition Program (NADP) including the wet-deposition concentration

397   and loading of NH_4^+, NO_3^-, PRISM precipitation deposition data at yearly time-scales across the

398   U.S., and dry deposition from EPA CASTNET data (EPA CASTNET, 2019; NADP, 2018;

399   Schwede & Lear, 2014). The composite TDEP produce is available as a smoothed, yearly (once

400   per year) gap-filled CONUS product for years 2000-2018 at 4km x 4km pixel sizes. From the

401   total TDEP deposition and the total stream losses (stream yields *Y(t)*) per area, we calculated the

402   watershed retention capacity by subtracting the yearly watershed yield *Y(t)* as losses (Kg/hectare)

403   from the yearly TDEP depositional inputs (Kg/hectare) (Equation 4) (Lovett et al., 2000).

404   Though we do not directly analyze biogeochemical mechanisms and confounding factors within

405   our study, we acknowledge that a critical insight from all the prior work is that biogeochemical

406   cycling within the watershed is potentially more important to long-term stream exports than

407   atmospheric N-deposition alone (Lovett et al., 2000; Lucas et al., 2016). Internal biogeochemical

408   cycling terms for vegetation sinks (V), soil sinks (S), and gaseous loss sinks (G) (Figure 1) are

20

409   biogeochemical terms not accounted for in the retention equation and represent the unknown

410   internal source/sink terms.

411

412   (4) Retention Capacity= Ret % $= \frac{Inputs-Losses}{Inputs} * 100 = \frac{TDEP-Yields}{TDEP} * 100$

413

414   NDVI, which was obtained from the NASA MODIS satellite, represents broad scale

415   measurements of vegetation productivity, and biomass density, and is important as a controlling

416   factor on nitrogen availability and uptake from deposition in forests. MODIS data are available

417   in a smoothed, gap-filled, monthly CONUS data product for years 2000-2015 with 250m x 250m

418   pixel sizes (Spruce et al., 2016). Land cover (LC) and land cover change (LCC) data were

419   obtained from the Multi-Resolution Land Characteristics (MRLC) consortium National Land

420   Cover Database (NLCD) and represents the total land cover type across the CONUS for years

421   2001, 2008, and 2016, as well as the total change between 2001 and 2016 and have 30 x 30 m

422   pixel sizes (MRLC NLCD, 2020; Yang et al., 2018). We did not calculated trends from LC,

423   rather we used LC and LCC as a grouping variable. Elevations were obtained from a CONUS

424   scale digital elevation model (DEM) 1km x 1km pixel sizes (Maurer, 2016; Maurer et al., 2004).

425   Associated elevation categories (Elev groups) are defined as such: Low Elevation < 30m,

426   Medium Elevation (30-300m), Moderate Elevation (300-1500m), High Elevation > 1500m.

427   Elevations categories represent arbitrary cutoffs. Seasonal trends were calculated by aggregating

428   three month increments into each season: spring (March-April-May), summer (June-July-

429   August), fall (September-October-November), and winter (December-January-February). It is

430   unknown what the error of these products are.

431   We calculated yearly and seasonal trends for all variables, and compared the trends

432   accordingly across different TDEP, NDVI, LC, and Elev groups. TDEP-NDVI grouping

433   categories in Figure 2 were used to represent distinct regions with unique watershed stages of N-

434   saturation. We used the Kruskall-Wallis test for statistical significance between groups of data

435   such as *Ex* trends across Elev categories, or *Cn* trends across all increasing or decreasing NDVI

436   groups. All variable names, trend short-hand notation, and trend units used in this study are

437   shown in Table 2.

438

439   Table 2: Table of variables used, units, symbols to represent the variable and the relevant trend

440   (slope) units.

441

Variable	Units	Symbol	Time-Series	Slope (β or βMK)	Slope Units
Concentration	mg/L	C	$C(t)$	ΔC	mg/L/year
Discharge	m³/s	Q	$Q(t)$	ΔQ	m³/year
Export	Kg/day	E	$E(t)$	ΔE	Kg/year or Mg/year
Yield	Kg/km²/day	Y	$Y(t)$	ΔY	Kg/ha/year or Mg/ha/year
Flow Normalized Concentration	mg/L	FNC	$FNC(t)$		mg/L/year
Flow Normalized Export	Kg/d	FNE	$FNE(t)$		Kg/year or Mg/year
Flow Normalized Yield	Kg/km²/day	FNY	$FNY(t)$		Kg/ha/year or Mg/ka/year
Normalized Differenced Vegetation Index	unitless	$NDVI$	$NDVI(t)$	$\Delta NDVI$	"-"/year
Total Wet+Dry Nitrogen Deposition	Kg/ha	$TDEP$	$TDEP(t)$	$\Delta TDEP$	kg/ha/year
Elevation	m	$ELEV$			

442

443

444   **2.4 Watershed Aggregation**

445   Once station-based statistics, models, and trends were constructed, the slope values and the

446   statistics were aggregated to the different hydrologic unit code (HUC) 2-8 scales. When

447   aggregating trends from the station to the larger HUC2-HUC8 scales, we used two approaches:

448   *Simple averaging:* We used simple averaging of trends across all stations to get the

449   aggregated HUC2-HUC8 trends. We used this approach to map average trends in ΔE, ΔC, ΔY

450   and ΔQ. For example, all station slopes (β) for concentration were averaged for each HUC8

451   region to provide an average slope for that HUC8 region. When averaging the Q data for each

452   WQP, we averaged using only the stations where the particular WQP values were available.

453   When aggregating the Q data to the basin or watershed scales, we used all available Q data

454   across all WQP for that basin. We evaluated the significance of these trends by counting the

455   number of stations within each watershed that were statistically significant at $p < 0.05$.

456   Additionally, we averaged only statistically significant station trends across groups: TDEP-

457   NDVI groups, elevation groups, and land cover.

458   *Area-Weighted averaging:* Area-weighted averaging is a method of aggregating values by

459   applying weight to the values based on another variable. We calculated area-weighted averages

460   by weighting the trend values using contributing drainage areas such that exports from larger

461   contributing areas provide more weight to the average than exports from smaller contributing

462   areas. For example, when calculating the area-weighted average concentration for a HUC8

463   region, downstream concentrations have more weight applied in the averaging step than

464   upstream concentrations.

465   Statistical significance of trends was obtained from the previously described approaches:

466   linear correlation (Equation 2), Mann-Kendall tests, Hurst Exponent Persistence for each $C(t)$,

467    $Q(t)$, $Y(t)$, and $E(t)$ trend for each water parameter, and for each environmental variable of

468   interest (NDVI, TDEP, LC, Elev, Temp). Statistical significance was assessed at the p<0.05

469   value for linear model derived slopes (β), and for Mann-Kendall slopes (β_{MK}), and at the Hs>0.6

470   level for Hurst Persistence significance. To aggregate the statistical significance from the station

471   scale to the HUC 2-8 scale, we used a station thresholding approach to identify how many

472   watersheds contain more than 50% of stations with statistically significant and directionally

473   similar trends in ΔE and ΔC, or ΔE and ΔQ. We compared trends in station ΔE, ΔC, ΔY, and ΔQ

474   and counted the number of stations showing statistically significant (p<0.05) and directionally

475   similar trends (positive or negative) in these variables for every HUC2-HUC8 watershed. We

476   also used this approach to quantify the number of watersheds within four categories: similar ΔE-

477   ΔC trends, opposite ΔE-ΔC trends, similar ΔE-ΔQ trends, and opposite ΔE-ΔQ trends to evaluate

478   the role of concentration and discharge on long-term trends. We counted how many stations, and

479   what percentage of stations within each HUC2-HUC8 watershed fall in the four TDEP-NDVI

480   grouping categories. Because this CONUS 'big-data' approach requires a significant amount of

481   computational capabilities, all data processing and analysis was performed on the LBNL NERSC

482   supercomputer CORI cluster. We used over 30000 core hours requiring over 500Gb of memory

483   on the Cori 'Big-Memory' node and analyzed over 1Tb of data.

484

485   **3.0 Results**

486   Our results section is structured as follows: we first present results of the trend analysis for

487   TDEP, NDVI, and in-stream parameters for DIN, DOC, and Temp related to our first research

488   question (section 3.1, 3.2, and 3.3). We then examine how watershed exports and watershed

489   retention relate to the conceptualized TDEP-NDVI groups presented in Figure 2 to address our

490   second research question (section 3.4). Finally, we provide results examining potential

491 controlling factors on watershed retention including land use and elevation, and describe the

492 modalities of watershed retention hysteresis and one-way transition patterns (section 3.5 and

493 3.6).

494

495   **3.1 TDEP-NDVI Grouping Classification**

496   Considerable spatial variability in TDEP and NDVI trends is found across the CONUS

497 (Figure 3). General patterns across a few HUC2 scales are highlighted. In HUC2 basin #10

498 (Missouri Basin), patterns of increasing NDVI and increasing TDEP (Group a) reflect the

499 majority of HUC8 scale watersheds within the Missouri. Across the South Atlantic-Gulf Basin

500 (HUC2 #03), increasing trends in NDVI are associated with decreases in TDEP (Group c). In the

501 Ohio Basin (HUC2 #05), decreasing patterns of NDVI are observed with decreasing patterns in

502 TDEP (Group d). Across the Pacific Northwest Basin (HUC2 #17), spatial variability in N-

503 saturation groups are found with regions showing difference in TDEP and NDVI. Many HUC8

504 regions within the Pacific Northwest fall into Group b, representing increases in TDEP and

505 declines in NDVI. Across the CONUS, 50% of HUC8 watersheds fall into Group a, 20% in

506 Group b, 20% in Group c, and 10% in Group d. We use the TDEP-NDVI groupings throughout

507 the rest of the paper to facilitate interpretation of watershed N-losses and N-retention trends.

508 TDEP-NDVI groups and their conceptualized role on in-stream trends are provided in Figure 2.

509
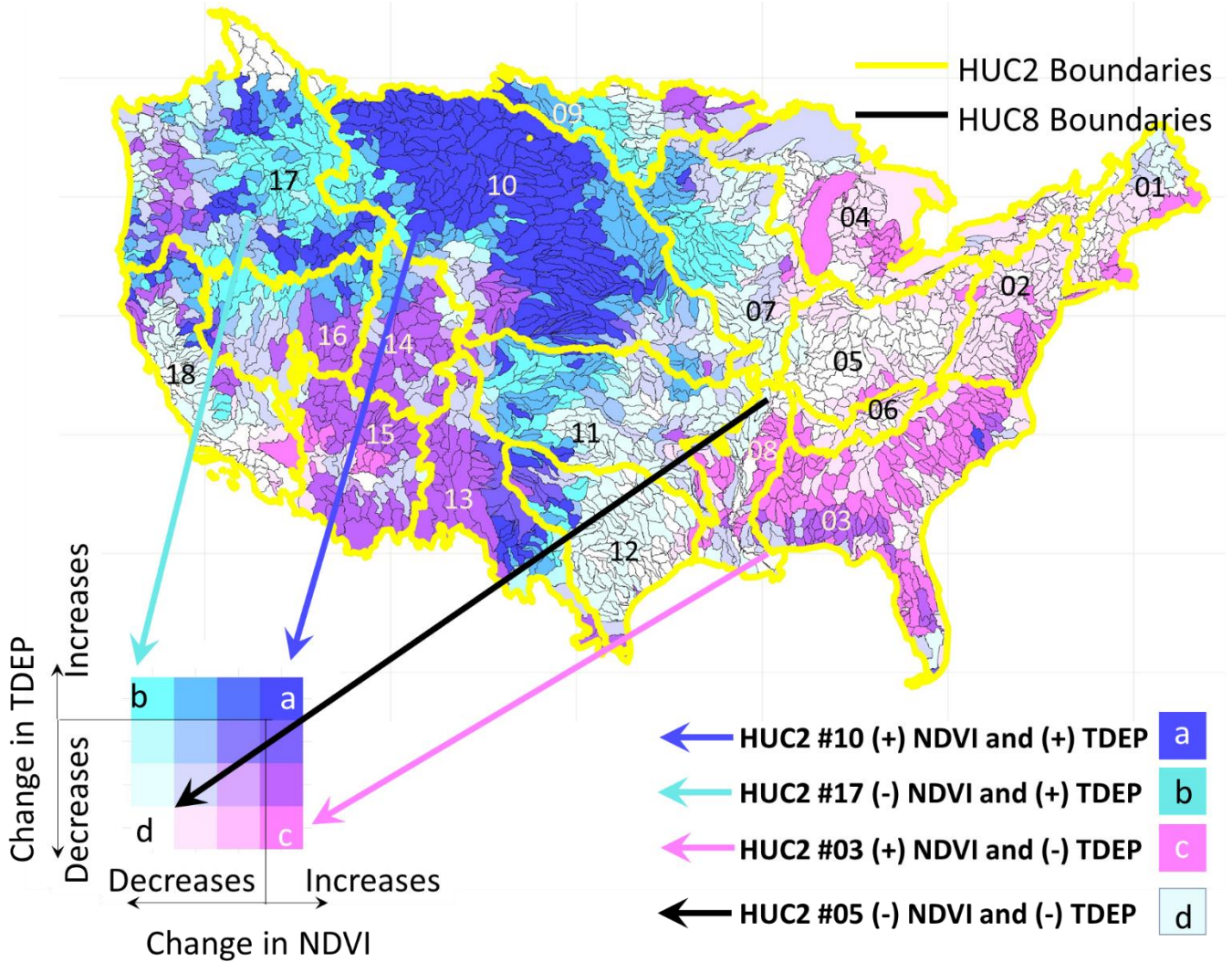
Figure 3: Groupings and directionality of vegetation and deposition change based on trends in

TDEP (2000-2018) and NDVI (2000-2015). Groupings include: : Group a) regions with

increasing NDVI and increasing TDEP, Group b) regions with decreasing NDVI and increasing

TDEP, Group c) regions with increasing NDVI and decreasing TDEP, and Group d) regions with

decreasing NDVI and decreasing TDEP. HUC2 boundaries are shown by the yellow line with

their corresponding HUC2 basin numbers. Groups a-d and their colors are used consistently

throughout the rest of this paper and refer to the same groups illustrated in Figure 2 and defined

in Section 1.0.

518

519

520   **3.2 Concentration Trends across US Basins**

521   CONUS-wide DIN concentration trends across HUC4 watersheds shows wide-variability

522   (Figure 4). All means are calculated from stations with statistical significance only. Statistical

523   significance was evaluated with the linear trend parameter, the Mann-Kendall trend parameter,

524   and the Hurst persistence parameter. Across the CONUS, 36.5% of stations show statistically

525   significant declining concentrations of DIN (-0.005 ± 0.004 mg/L/year), while 38.1% of stations

526   show statistically significant increasing concentrations of DIN (+0.0082 ± 0.0092 mg/L/year). It

527   is common for water quality datasets to have such large standard deviations because of

528   interannual variability (i.e. (Strauss et al., 2004)). We highlight six HUC2 watersheds, four from

529   Figure 3 (HUC2 #03, HUC2 #05, HUC2 #10, HUC2 #17) which represent the Groups a-d, and

530   two additional HUC2 watersheds to contrast results (HUC2 #14, and HUC2 #12). Tables of DIN

531   concentration statistics for these six watersheds are provided in Supplementary Table B1. Of

532   these six basins, we find the largest DIN concentrations across the Texas Gulf Basin (HUC #12)

533   (1.88 ± 3.04 mg/L), with average increasing rates of change ($\beta = 0.007 \pm 0.053$, $\beta_{MK} = 0.01 \pm$

534   0.068 mg/L/year). These rates contrast basins such as the Upper Colorado HUC #14 (0.33 ± 0.57

535   mg/L), 49.1% of stations show statistically significant trends and show a declining rate of change

536   ($\beta = -0.007 \pm 0.027$, $\beta_{MK} = -0.003 \pm 0.026$ mg/L/year). The Upper Colorado has the lowest

537   concentrations of DIN among the six basins. In the Ohio Basin (HUC2# 05), average DIN

538   concentrations are 1.78 ± 3.38 mg/L. The Ohio Basin shows the largest average rates of decline

539   with a majority of stations (nSLP/nS >50%) showing statistically significant downward trends (β

540   = -0.03 ± 0.14 mg/L/year, $\beta_{MK} = -0.04 \pm 0.18$ mg/L/year). The number of stations showing

27

541   significance of Mann-Kendall trend parameters generally agrees with the significance of the

542   linear parameter (nSLP ≈ nSMKP). Trend statistical significance calculated with the Hurst

543   Persistence parameter shows a larger fraction of stations have persistent trends than the linear or

544   Man-Kendall parameters (see for example HUC#10, nSH = 251). Tables of statistics for all other

545   HUC2 watersheds, statistical significance, linear, and Mann-Kendall trends are also provided in
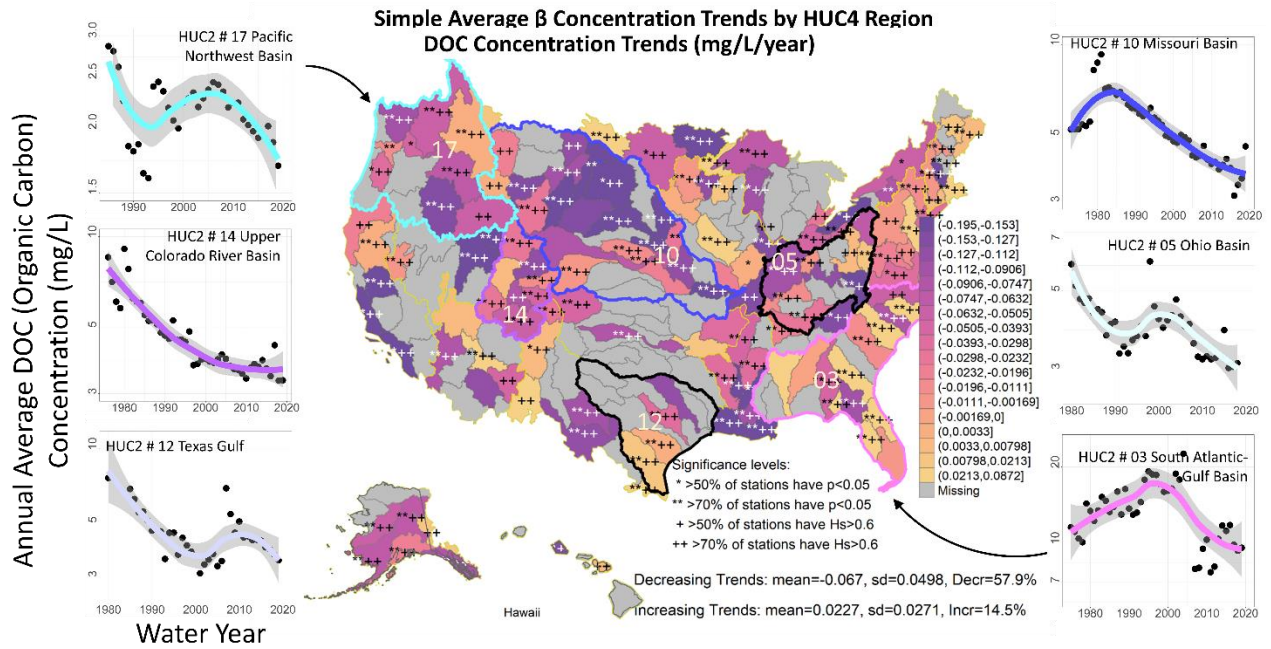
546   Supplementary Table B1.

547

548

549   Figure 4: Trends in DIN concentrations *C(t)* from 1970-2020 for the CONUS and select HUC2

550   basins #17, 14, 12, 10, 05, and 03 are shown with the same colors corresponding to the groupings

551   in Figure 3. Trends are shown from the average gap-filling method and β trends calculated for

552   each station and aggregated up using Simple Averaging. Trends statistics are provided in

553   Supplementary Table B1. Average annual DIN concentrations over time are shown for the

554   selected six HUC2 basins. Significant levels are indicated by the following symbols: * >50% of

555   stations have p<0.05, **>70% of stations have p<0.05, + >50% of stations have Hs>0.6, and ++

556   > 70% of stations have Hs>0.6.

557

558   Similarly, across the CONUS we find increasing and decreasing trends in DOC

559   concentrations for the different HUC2 and HUC4 basins from 1970-2020 (Figure 5), however

560   major gaps in DOC coverage occur across the CONUS. On average, 57.9% of HUC4 watersheds

561   show statistically significant decreasing concentrations (-0.067 ± 0.049 mg/L/year), while 14.5%

562   of HUC4 watersheds show statistically significant increasing concentrations (0.022 ± 0.027

563   mg/L/year). We find the largest DOC concentrations across the South-Atlantic Gulf Basin (HUC

564   #03) (13.36 ± 13.79 mg/L), with the lowest rates of DOC change ($\beta = 0.037 \pm 0.33$, $\beta_{MK} = 0.035$

565   ± 0.34 mg/L/year). In the Missouri Basin HUC #10, average concentrations (5.78 ± 4.65 mg/L)

566   are coupled with the largest rates of DOC concentration change ($\beta = -0.080 \pm 0.13$, $\beta_{MK} = -0.081$

567   ± 0.17 mg/L/year). Tables of statistics for all other HUC2 watersheds, statistical significance,

568   linear, and Mann-Kendall trends are also provided in Supplementary Table B2. We also provide

569   trend maps for all other water parameters in Supplementary Figure B1-B2. Temperature maps

570   with the same selected six HUC2 basins (Supplementary Figure B3) and temperature statistics

571   are also provided (Supplementary Table B3).

572
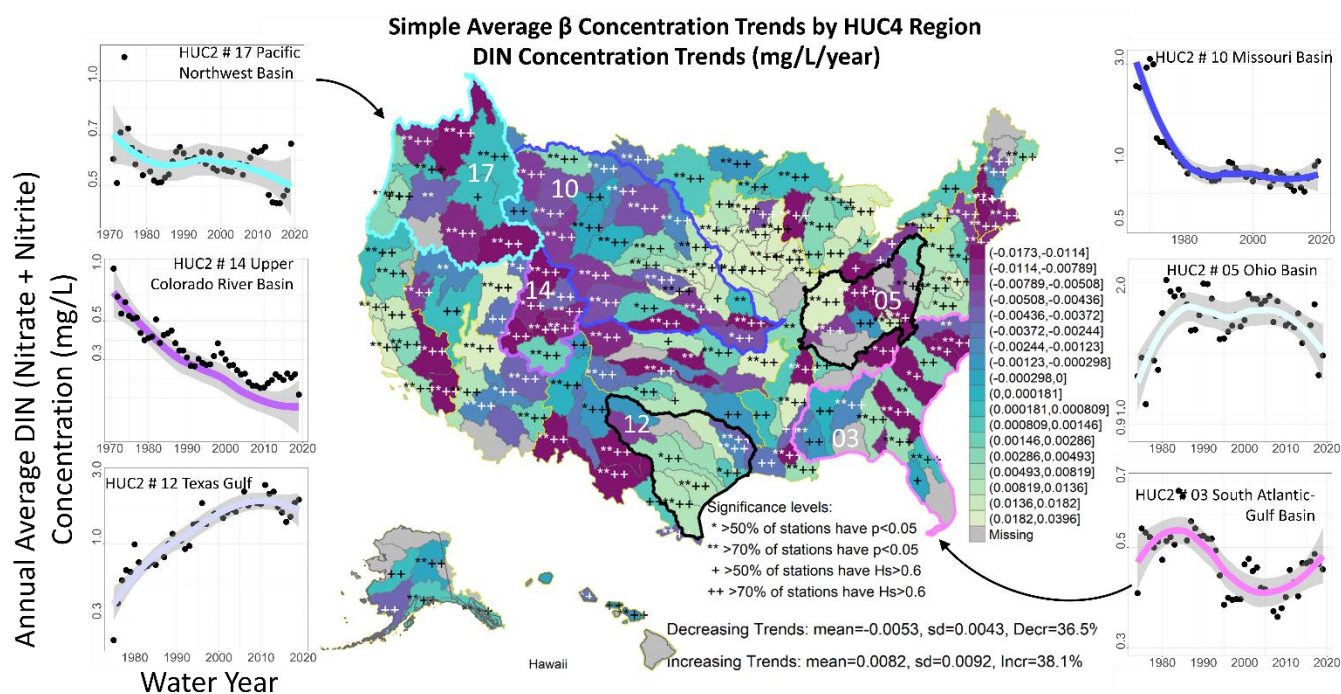
Figure 5: Trends in DOC concentrations *C(t)* from 1970-2020 for the CONUS and select HUC2

basins #17, 14, 12, 10, 05, and 03 are shown with the same colors corresponding to the groupings

in Figure 3. Trends are shown from the average gap-filling method and β trends calculated for

each station and aggregated up using Simple Averaging. Trends statistics are provided in

Supplementary Table B2. Average annual DOC concentrations over time are shown for the

selected six HUC2 basins. Significant levels are indicated by the following symbols: * >50% of

stations have p<0.05, **>70% of stations have p<0.05, + >50% of stations have Hs>0.6, and ++

> 70% of stations have Hs>0.6.

581

3.3 The Role of Trends in Discharge on Trends in Exports across US Basins

Calculations of DIN exports (watershed losses) represent the combined effect of discharge

and concentration in a basin (Equation 1) and are directly used in the calculation of watershed N-

retention (Equation 4). *Trends* in DIN exports (linear β parameter for *Ex(t)* Mg/year) across all

30

586   U.S. stations, aggregated to U.S. HUC4 watersheds show patterns of spatial variability in the

587   direction (increasing or decreasing) and statistical significance similar to concentration trends

588   (Figure 4, Supplementary Figure B4). We found 34.8% of all stations (nS = 1136) across

589   CONUS showed statistically significant decreasing trends in DIN exports (β = -3.2 ± 4.2

590   Mg/year, outliers > 99th percentile and < 1st percentile removed) (Supplementary Figure B4A).

591   Another 22.3% of CONUS stations show statistically significant increasing DIN export trends (β

592   = 8.4 ± 13.9 Mg/year, outliers > 99th percentile and < 1st percentile removed). Aggregating all of

593   the station export data *Ex(t))* to all the HUC2 levels shows similar variability in magnitude and

594   distribution of DIN export change across the CONUS (Supplementary Table B4, Supplementary

595   Figure B5). Tables and maps of discharge, exports and their statistics are provided in

596   Supplementary Figures B6-B9 and Tables B4-B7).

597   Trends in watershed exports are not only important for determining watershed retention

598   metrics, but also for characterizing future changes in N and C deliveries to coastlines. The

599   magnitude and direction of DIN export *trends* relative to the magnitude of yearly exports ranges

600   between -16 – 24% per decade (all HUC2 decadal changes are provided in Supplementary Table

601   B4). HUC #14, for example, shows a decline in DIN exports of -16.9% over the next decade,

602   which is the largest declining rate relative to the other HUC2 basins, albeit quite low in

603   magnitude (-66.9 Mg over the next decade). By comparison, HUC #17 also shows a decline in

604   DIN exports of -4.6% over the next decade but a much larger magnitude (-127.7 Mg over the

605   next decade). We aggregated these annual estimates of DIN and DOC trends to calculate total

606   coastal exports from the land to the ocean from coastal abutting basins (specifically HUC2 #01,

607   02, 03, 08, 12, 13, 15, 17, 18, 19, 20). Across the coastal basins directly exporting N and C to the

608   ocean, we found annual average coastal N and C exports are declining. Total dissolved inorganic

609   nitrogen exports (sum of filtered nitrate, nitrite, ammonia, ammonium) have declined by

610   approximately 60% over the past two decades (1970-2000: 9.4 Tg-N/year, 2000-2020: 3.72 Tg-

611   N/year), and organic carbon exports have declined by approximately 80% over the past two

612   decades (1970-2000:19.5 Tg-C/year, 2000-2020: 3.72 Tg-N/year).

613   While discharge is always the most significant contributor to yearly export magnitudes on an

614   inter-annual basis, we found no conclusive evidence that decadal *trends* in discharge are the most

615   significant contributor to decadal *trends* in exports (Figure 6). We found statistically significant

616   discharge trends at < 10% of all CONUS stations (Supplementary Figure B9, Table B5).

617   Correlations between trends in $Cn(t)$ and $Ex(t)$ were statistically significant at the p<0.001 level

618   (Figure 6 a,b) while correlations between trends in $Qs(t)$ and $Ex(t)$ were statistically significant at

619   the p=0.04 level (Figure 6 c,d). We observed that while changes (*trends*) in DIN and DOC

620   exports are driven by *both* concentration and discharge (Supplementary Figure B10, B11),

621   changes in exports were more often associated with changes in concentration rather than

622   discharge (Supplementary Table B8). When correlating decadal *trends* in discharge and

623   concentration to *trends* in exports for all water parameters, we found directionally similar and

624   statistically significant trends in $Cn(t)$ and $Ex(t)$ across more than 25% of stations. Conversely,

625   we found directionally similar and statistically significant trends in $Qs(t)$ and $Ex(t)$ at <3% of

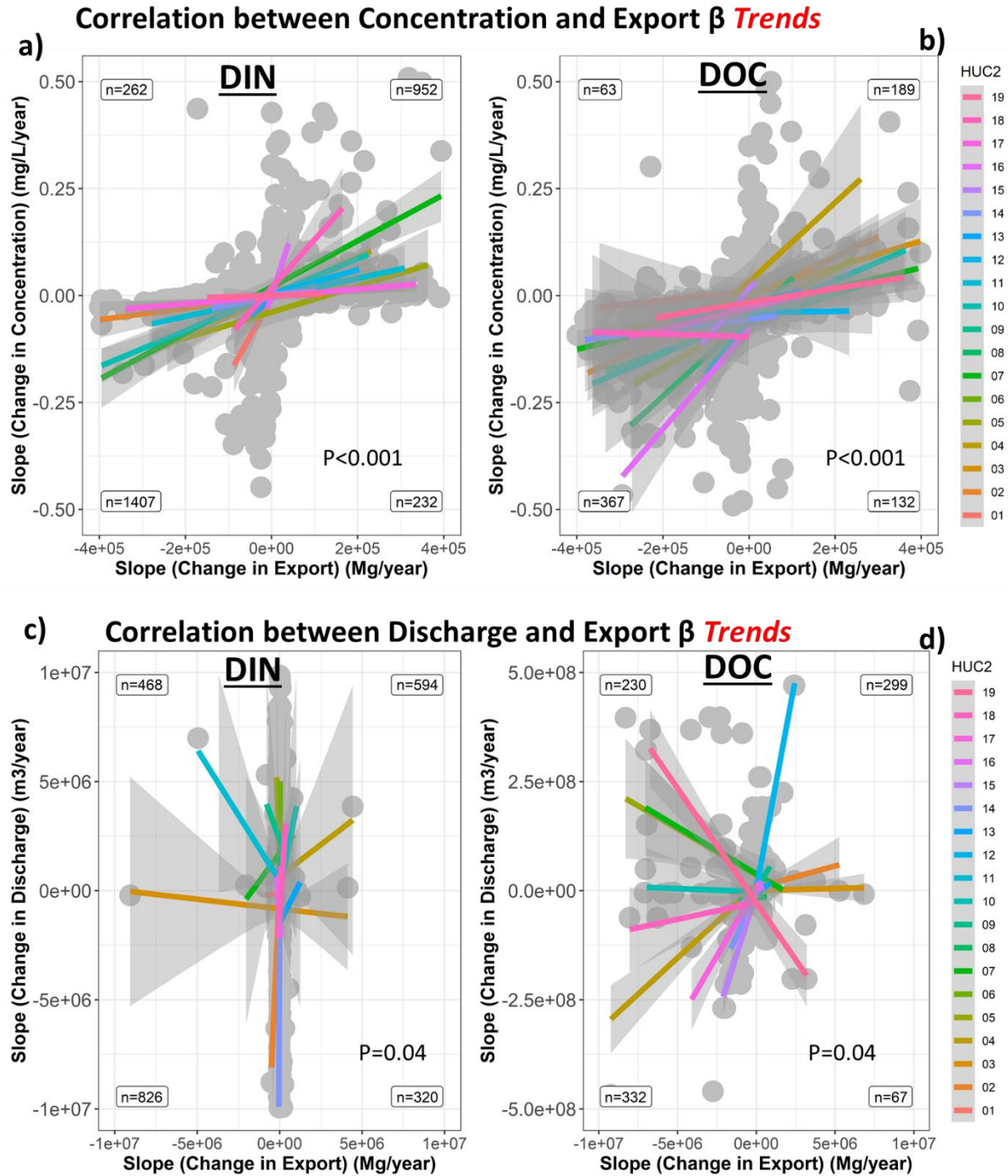626   stations (Supplementary Table B8).

627

628

Figure 6: Correlations between trends in concentration and exports (a, b) and correlations between trends in discharge and exports (c,d) for DIN and DOC and each HUC2 basin shown by the various colors. Total statistical significance for the trends is provided in each figure. Each quadrant shows the number of stations (n) that fall within each quadrant.

33

634

635

636   **3.4 Trends in Watershed Exports for NDVI-TDEP Groups**

637   We examined trends in watershed exports across the NDVI-TDEP Groups to examine the

638   degree to which CONUS scale atmospheric deposition patterns, vegetation trends, and stream

639   trends can be potential indicators of watershed N-retention conditions conceptualized in our

640   watershed hysteresis model (Figure 2). Trends in $E(t)$ (Mg/year) for DIN and DOC obtained

641   from all stations and aggregated by NDVI-TDEP groups from Figure 3 show distinct trends that

642   support our conceptual model (Figure 7). DIN shows similar modes of variability across the

643   TDEP-NDVI groups for both exports and yields: greater declines in exports (mean β = -9.97 $\pm$

644   148.5 Mg/year) and yields (mean β = -0.001 $\pm$ 0.04 Kg/hectare/year) in Group a, with steady

645   increases across the TDEP-NDVI groups towards increasing exports (mean β = 59.08 $\pm$ 148.8

646   Mg/year) and yields (mean β = 0.13 $\pm$ 0.56 Kg/hectare/year) in Group d. DIN export trends in

647   Group a (declining trends) are associated with in-stream concentration declines (-0.0016

648   mg/L/year $\pm$), and DIN export trends in Group d (increasing trends) are associated with in-

649   stream DIN concentration increases (+0.0052 mg/L/year $\pm$) (colors in Figure 7 indicate

650   concentration trends). DIN export trends show statistically significant differences between

651   Groups a-d (K.W. p=0.0015). DOC export trends are statistically significant between groups

652   (K.W. p=0.0055) and show an interesting pattern of reversal from Group a to d: declines in

653   exports are found for Group a and Group d (Group a mean β = -444 $\pm$ 574 Mg/year, Group d

654   mean β = -854 $\pm$ 2253 Mg/year), but a greater proportion of increasing trends are found in Group

655   b (mean β = 115 $\pm$ 114 Mg/year). DOC concentrations are declining for all groups except for

656   Group c (0.0011 mg/L/year). Trends in $E(t)$ (Mg/year) and $Y(t)$ (Kg/hectare/year) by NDVI-

657 TDEP group for all water parameters are provided in Supplementary Figure B12. Seasonally

658 aggregated barplots are provided in Supplementary Figure B13.
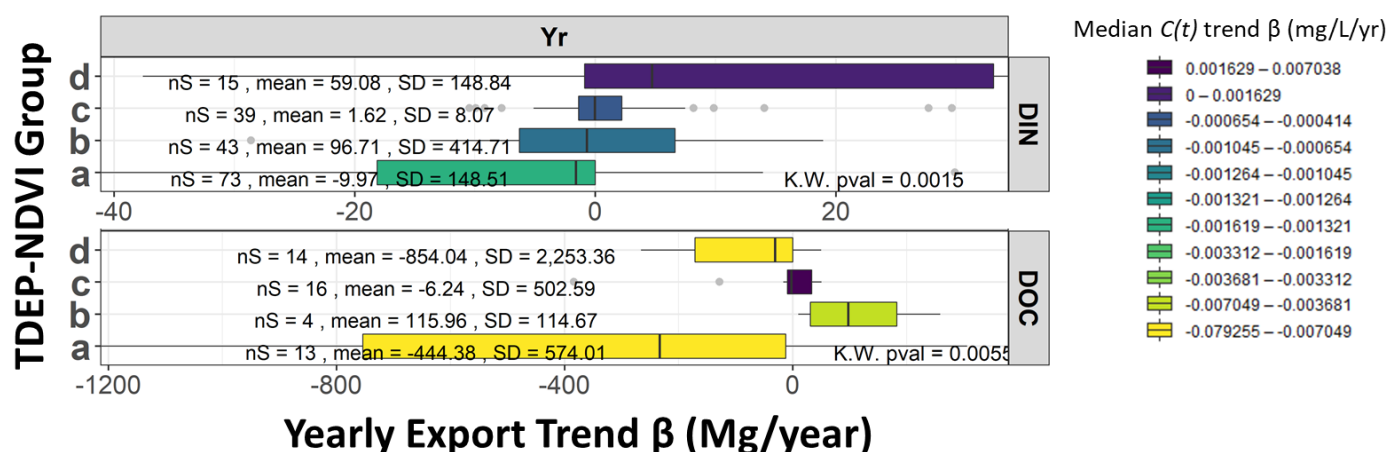
659

660

661

662 Figure 7: Box plots of the export and yield data separated by WQP and NDVI-TDEP groups.

663 Boxplots show the median as the middle line, upper (75%) and lower (25%) quartiles as ends of

664 the box, and upper and lower fences representing 1.5 times the inter-quartile range. If there are

665 outliers more or less than 1.5 times the upper or lower quartiles, respectively, they are shown

666 with grey dots. All trend results are colored based on the associated median trends in $C(T)$.

667 Colors represent median values of concentration change for that box (mg/L/year). The number of

668 statistically significant stations (nS), the mean and standard deviation are shown next to each

669 box. All statistics were calculated using only stations with statistically significant trends

670 (p<0.05). As a reminder of the TDEP-NDVI grouping representations, Groups a (+TDEP,

671 +NDVI), Group b (+TDEP, -NDVI), Group C (-TDEP, +NDVI), and Group d (-TDEP, -NDVI).

672

673 **3.5 Retention across U.S. Basins**

35

674   Watershed retention (Equation 4, TDEP inputs minus watershed exports) of atmospheric

675   TDEP across all U.S. HUC4 basins reveals wide variability in retention patterns (Figure 8) when

676   compared by region or NDVI-TDEP group. The lowest retention values across the CONUS

677   occur in the Midwest region (HUC2 #07 mean retention = 35%) (Figure 8 a,b, Supplementary

678   Table B8). By contrast, most regions across the U.S. have high watershed N-retention (>90%)

679   and sustain high retention values before 2007 (Figure 8a) and after 2007 (Figure 8b) (2007 is an

680   arbitrary year to evaluate temporal trends by comparing means). Retention calculations across

681   CONUS also reveal differences when assessed between NDVI-TDEP groups (Figure 8c). Most

682   HUC8 watersheds classified as Group a, retain close to 100% of incoming atmospheric TDEP

683   (median = 98.6%, mean = 93.3%, s.d. = 17.6%) (Figure 8c). Watersheds classified within Group

684   d retain about one-half to two-thirds of incoming TDEP (median = 77.8%, mean = 61.8%, s.d. =

685   42.1%). As expected based on the proposed conceptual model (Figure 2), once watersheds

686   become N-saturated (occurs around Group b), retention of incoming N-deposition decreases and

687   more is lost directly to watershed exports leading to lower retention values (Groups c and d).

688   Retention statistics calculated for each HUC2 basin are provided in Supplementary Table B8.
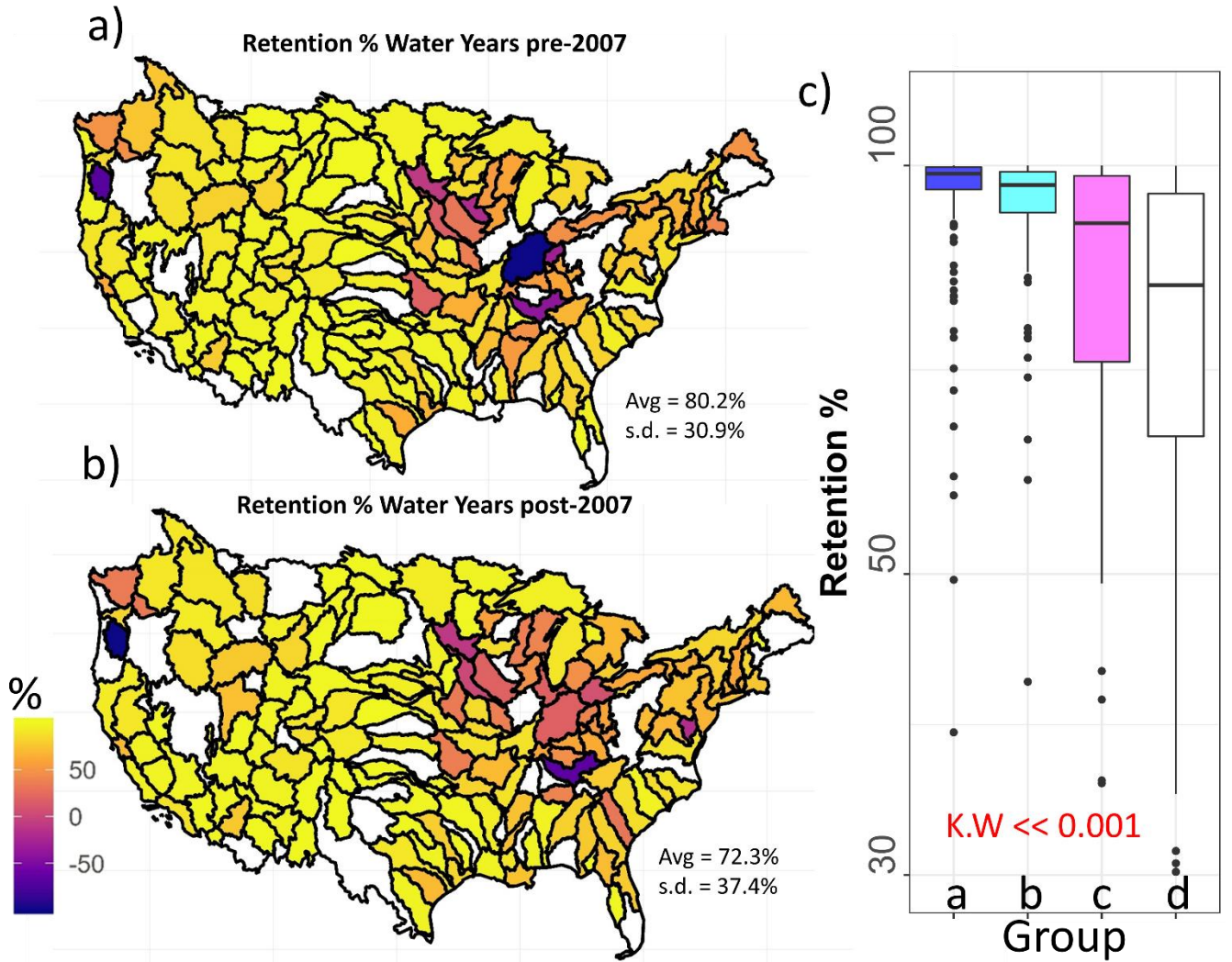
689

690

Figure 8: a) Spatial distributions and averages of retention (% Retention) are shown for HUC4

watersheds across the CONUS before 2007, b) Spatial distributions and averages of retention are

shown for HUC4 watersheds across the CONUS after 2007, c) Box plots of retention are shown

for the different TDEP-NDVI groups and show statistically significant differences (K.W. <<

0.001). As a reminder of the TDEP-NDVI grouping representations, Groups a (+TDEP, +NDVI),

Group b (+TDEP, -NDVI), Group C (-TDEP, +NDVI), and Group d (-TDEP, -NDVI).

697

698

699   Across HUC8 watersheds, retention is found to vary as a function of land-use

700   characteristics and NDVI-TDEP groups (Figure 9). Retention varies across the different NDVI-

701   TDEP groups in a similar fashion to that shown in Figure 8 with larger retention values on

702   average in Group a (92.5% ± 19.5 %) and lower retention values in Group d (61.1% ± 40.6 %).

703   For each land-cover class, K.W values for differences between NDVI-TDEP groupings are

704   statistically significant. Forest land cover shows highly variable retention across the NDVI-

705   TDEP groups with the lowest retention found in Group b (-13.0% ± 36.9 %). The negative value

706   for Group b indicates an additional source of N is present (outputs > atmospheric inputs). Planted

707   land-cover types, which include cultivated crops and pasture/hay also show a general decline in

708   retention from Group a (91.9% ± 20.5%) to Group d (51.5% ± 43.5%), but with much larger

709   distribution of values in Group b. Wetland land cover types show close to 100% retention for

710   NDVI-TDEP Groups a and b, and then trend downward for Groups c and d. Maximum land-

711   cover types and changes by HUC2 basin are provided in the Supplementary Figure B14.

712   Maximum land-cover types and changes by NDVI-TDEP group and year are provided in the

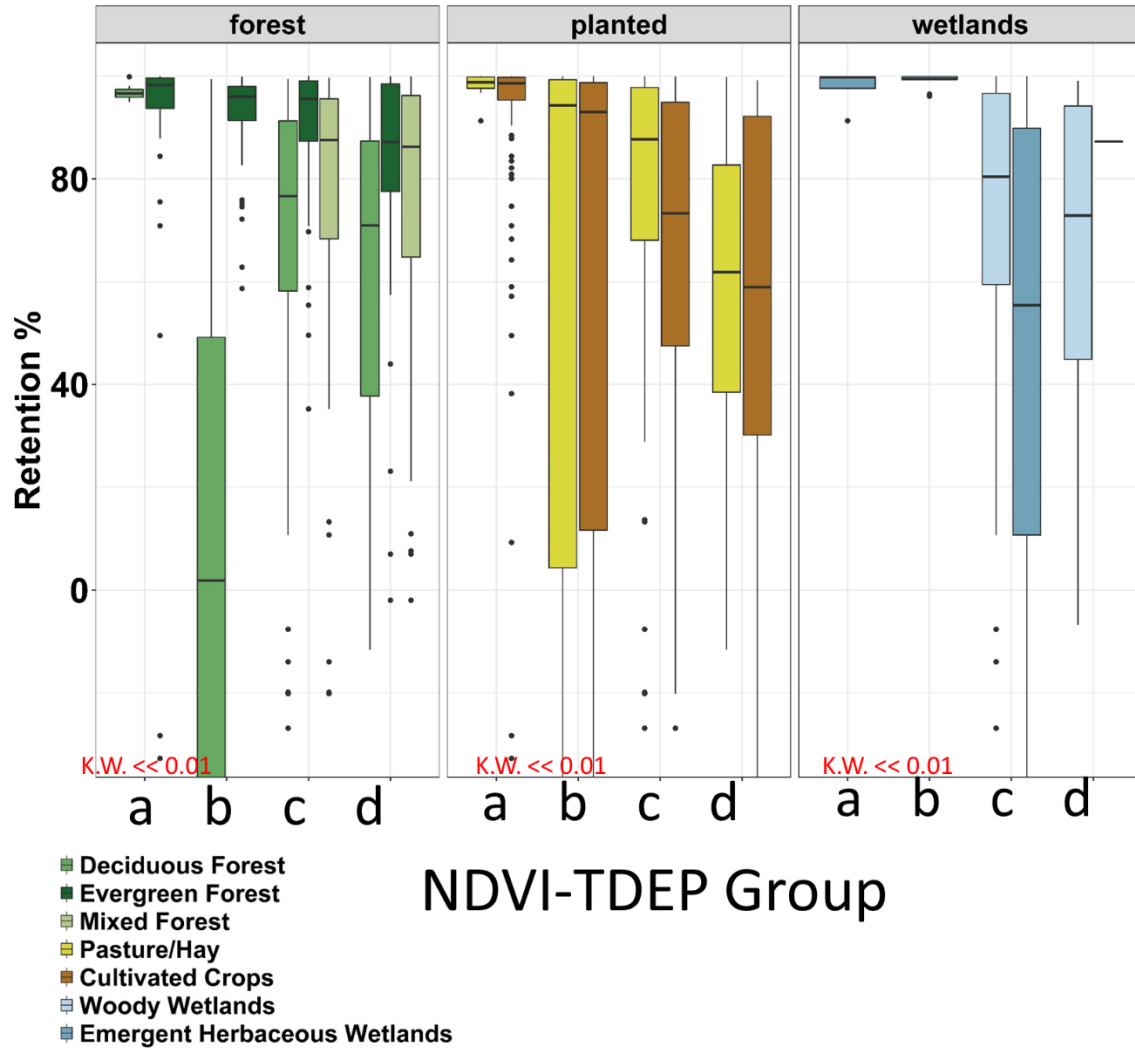713   Supplementary Figure B15.

714

715

Figure 9: N-retention across NDVI-TDEP groups and further refined by different land cover

class and types (forest, planted, and wetlands). Colors represent the different land-cover groups

within each broad land-cover class.

Comparing the total percent of variance in watershed N-retention explained by the four

groups of interest (land cover, NDVI-TDEP group, Elevation, and stream factors which include

stream temperature/DOC concentrations), our results indicate that land cover may not be the

primary controlling factor on watershed N-retention (Table 3). The total percent of variance in

726   watershed N-retention explained by land cover type ranges between 0.15-30.8 % (average

727   9.97%) which is the third largest factor among the four explanatory groups. NDVI-TDEP groups

728   primarily explain, on average a greater percent of the variance in watershed N-retention (range

729   4.03-45.14%, average 16.13%). Stream factors which include the combined temperature and

730   DOC concentration dataset explain the second largest percent of variance in watershed N-

731   retention (range 0.04-36.85%, average 13.23%). Regionally, land cover is a second order control

732   within the Lower Mississippi River basin (HUC 08, explains 30.8% of variability in N-retention)

733   despite land cover being of lesser importance in the five other HUC2 basins that contribute

734   directly to the Lower Mississippi (Arkansas White Red HUC 11, Missouri HUC 10, Upper

735   Mississippi HUC 07, Ohio HUC 05, Tennessee HUC 06). The Mid-Atlantic Basin (HUC #02) is

736   the only basin where land cover is identified as a primary co-variate to watershed N-retention.

737   The inclusion of the land-cover change dataset explained such a significantly low percentage of

738   variability (<0.0001%) that we do not show those results here and we excluded that variable

739   from the analysis.

740

741   Table 3: Percent of variability in watershed N-retention explained by the four different variables

742   of interest for each HUC 2 basin. The percent of variability explained by each variable was

743   calculated using the ANOVA statistical analysis and statistical significance of each variable is

744   indicated in parentheses.

745

Percent of Variability In Watershed N-Retention Explained

HUC	Maximum Land Cover Class	NDVI-TDEP Group	Elevation	Stream Factors (Temperature and DOC)
01	0.25(0.144)	11.69(0)	0.5(0.038)	19.82(0)
02	20.16(0)	6.51(0)	0.28(0.012)	11.49(0)
03	2.98(0)	15.91(0)	0.07(0.372)	6.88(0)
04	7.45(0)	12.52(0)	0.68(0.001)	11.39(0)
05	9.95(0)	12.27(0)	1.1(0.025)	11.19(0)
06	3.48(0.008)	17.12(0)	4.52(0.003)	13.12(0)
07	19.29(0)	34.83(0)	0.09(0.14)	5.47(0)
08	30.8(0)	45.14(0)	0(0.862)	12.53(0)
09	8.08(0)	35.4(0)	5.79(0)	6.08(0)
10	9.19(0)	11.09(0)	4.03(0)	6.89(0)
11	11.94(0)	16.95(0)	0.82(0)	3.55(0)
12	14.57(0)	4.03(0)	0.21(0.095)	21.73(0)
13	0.16(0.398)	4.77(0)	2.11(0.002)	12.78(0)
14	10.07(0)	6.74(0)	1.6(0)	32.64(0)
15	5.92(0)	17.56(0)	29.39(0)	4.57(0)
16	1.72(0.002)	19.13(0)	1.61(0.003)	24.89(0)
17	0.87(0)	16.8(0)	0.45(0)	36.88(0)
18	22.75(0)	6.91(0)	0.98(0)	31.74(0)
Average	9.97%	16.40%	3.01%	15.17%
	1	9	1	7

746 * p-values are shown in parentheses

747

748

749

750   **3.6 Modalities of Watershed Retention and Hysteresis**

751   TDEP and NDVI are important controlling factors on watershed N-retention patterns, and

752   our results demonstrate evidence for watershed N-hysteresis across the range of deposition

753   environments (Figure 10a). Watersheds with high retention capacity (where >90% of N is

754   retained, red dots) show a trend toward increasing NDVI with TDEP—watersheds with high

755   retention capacity have the potential to store excess N in biomass and likely become N-saturated

756   as TDEP increases (TDEP range 3-10 Kg/hectare/year, NDVI range 0.2-0.6, Figure 10a).

757   Watersheds with low retention capacity (<20% of N is retained, blue dots) are N-saturated or

758   undergoing recovery from N-saturation and show a different relationship with NDVI and TDEP

759   than the high-retention capacity group (Figure 10a). Low-retention watersheds undergoing

760   reversal from N-saturation show that NDVI remains high for all values of TDEP and appears to

761   decline quite significantly once TDEP is < 3 Kg/hectare/year. Our results show that the

762   relationship between NDVI and TDEP differs depending on how saturated the watershed is and

763   the state of NDVI and TDEP. Lower initial values of NDVI are associated with the increasing

764   NDVI group while larger initial values of NDVI are associated with the decreasing NDVI groups

765   (Figure 10c). Similarly with TDEP, lower values are within the increasing TDEP category, and

766   larger values are in the decreasing TDEP category (Figure 10b). Watersheds with a high N-

767   retention capacity are generally associated with regions of increasing TDEP and NDVI patterns,

768   while watersheds with a low N-retention capacity are generally associated with regions of

769   decreasing NDVI and TDEP patterns. As the first line of evidence supporting N-hysteresis in

770   watersheds, these generalizable patterns suggest that eventual recovery from excess N-deposition

771   may include a lagged response and a legacy of compromised forest health.
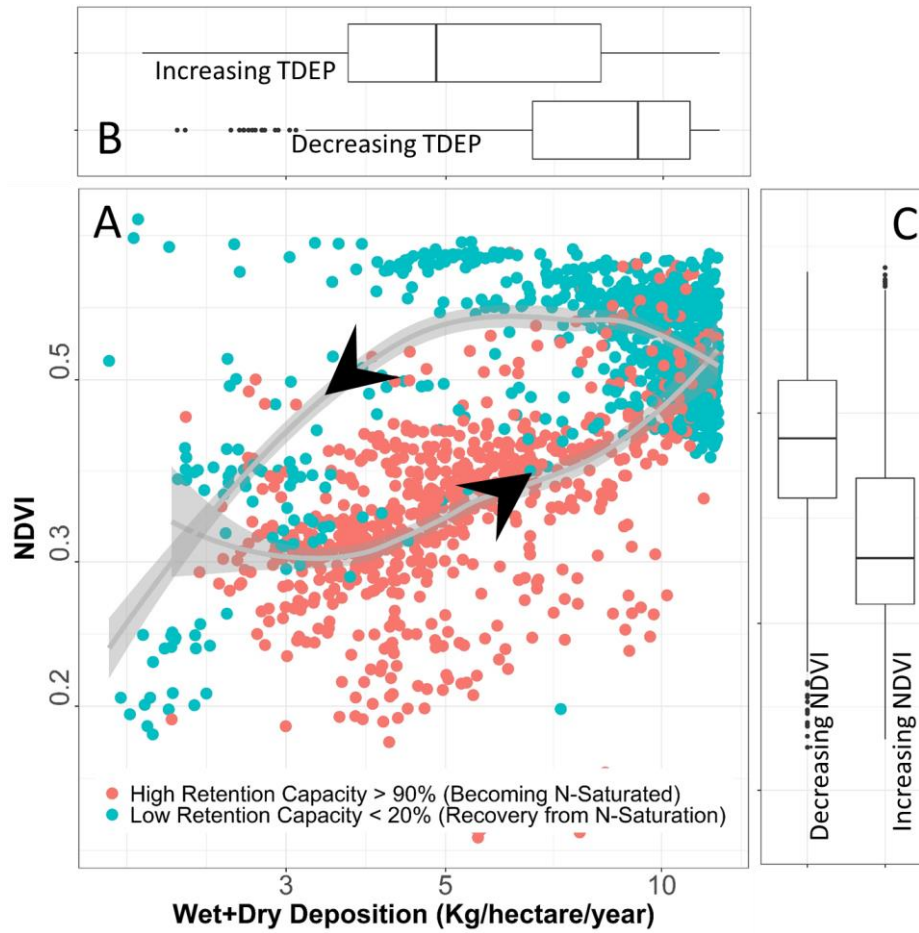
772

773

774

Figure 10: a) Scatterplot of NDVI and TDEP colored by high (red dots) and low (blue dots)

watershed N-retention capacity. High retention capacity watersheds are those that retain most

atmospheric deposition and have very low losses in stream exports. Low retention capacity

watersheds are those that lose most atmospheric deposition to stream losses. B) Boxplot

distribution TDEP values (associated with x-axis) grouped by trends in TDEP. C) Boxplot

distribution of NDVI values (associated with y-axis) grouped by trends in NDVI.

781

782

Hysteresis and one-way transition patterns of watershed N-retention and loss for a few

select individual HUC8 watersheds reveal varying modalities of N-retention and recovery are

785   possible (Figure 11). The highlighted watersheds with permanent changes (i.e. one-way

786   transition to a new steady-state) are represented by maximum land cover types of Evergreen

787   Forest-72.34% (permanent increase in retention, Figure 11a), and Deciduous Forest-38.08%

788   (permanent decrease in retention, Figure 11b). A transition from Evergreen Forest to Grassland

789   is observed (86.16% coverage in 2001 to 72.34% in 2016) and associated with a one-way

790   increase in retention and decreases in losses (Figure 11a). One-way declines in retention and

791   increases in losses are found in HUC8 #02080103 (Rapidan-Upper Rappahannock. Virginia)

792   with a dominant land cover type classified as Deciduous Forest (Figure 11b). The percent of the

793   dominant land cover class (Deciduous Forest) does not change much over the 2000-2016 time

794   period. Some land cover change does occur (-1.1% conversion of Pasture to Cultivated Crops,

795   Grassland) (Figure 11b). The watersheds with one-way increase and loss patterns (Figure 11a, b)

796   are notable because they potentially represent watersheds that have transitioned beyond an

797   equilibrium state in response to N deposition or other changes.

798   Clockwise and counterclockwise hysteresis patterns representing the systems recovery to

799   initial conditions also emerge (Figures 11c, d, e, f, g, h). In some cases, the watershed moves to a

800   new state represented by changes in both retention and loss (Figure 11c, e), or the watershed

801   returns to the original state represented by values of retention and loss that are at or near the

802   initial state (Figure 11f, g). This might be interpreted as having an unperturbed biogeochemical

803   cycling capacity such that it can sustain significant deviations from the original state and still

804   return to the original state. Watersheds with Retention ≈ 0% are rare (n=14 out of 2119 HUC8

805   watersheds) and represent watersheds with close to equal inputs (TDEP) and outputs (losses or

806   Yields), 3 of which occur in the Upper Mississippi (HUC2 #07). These watersheds either have a

807   significantly perturbed N-cycle due to some other anthropogenic factor and only represent a

808   steady state condition such that inputs = outputs. However, they could also represent a subset of

809   watersheds lacking significant biogeochemical capacity. Watersheds with outputs greater than

810   inputs are similarly rare, representing <5% of watersheds (n=103 out of 2119 HUC8

811   watersheds), 29 of which are in the Upper Mississippi (HUC2 #07). Watersheds representing

812   near pristine conditions, with retention close to 100%, represent ~12% of HUC8 watersheds

813   (n=251 out of 2119 HUC8 watersheds), 65 of which are in the Missouri Basin (HUC2 #10, 58%

814   Grassland/Herbaceous, Supplementary Figure B13). The rare, perturbed, and pristine HUC8

815   watersheds are listed in Supplementary Table B9. While we highlight individual watersheds

816   here, we also recognize many watersheds do not have clear patterns and require much greater

817   interrogation into underlying processes.

818

819
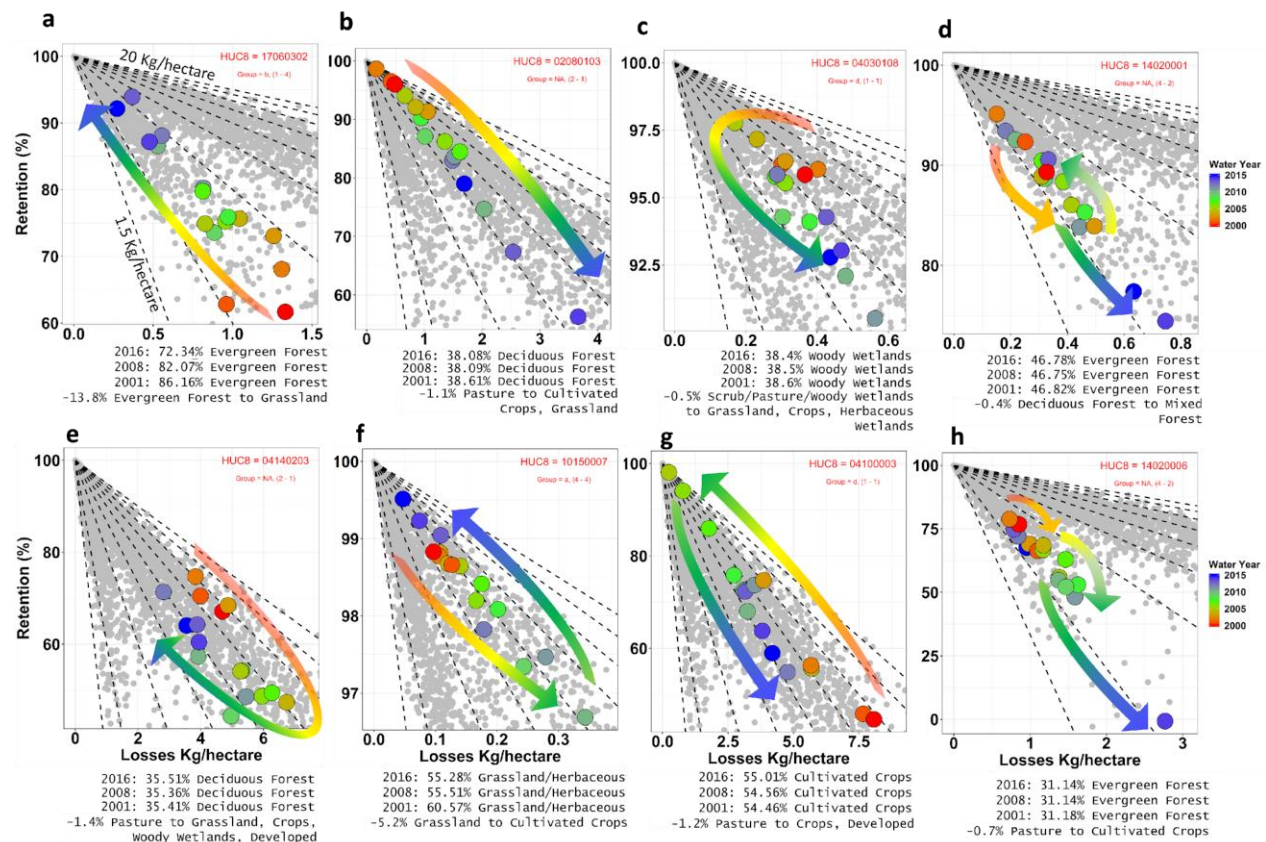
820   Figure 11: Scatter plots and hysteresis curves of HUC8 watershed retention (%) (y-axis) and loss

821   (x-axis) (Kg/hectare) in individual HUC8 watersheds. Dashed lines represent lines of equal

822   TDEP (Kg/hectare) ranging from 1.5-20 Kg/hectare. Colors represent the water year and are

823   increasing from the year 2000 (red) to 2015 (blue). Arrows are shown that follow the time series

824   of colors (red to blue representing the year 2000-2015) and show either the one-way transition or

825   the hysteresis pattern. If the arrow curves in a circular pattern, hysteresis is identified, but if the

826   arrow is uni-directional, then this is a one-way transition. Percentages below each figure

827   represent the land cover type with the maximum percentage coverage for each year.

828

829

830   **4.0 Discussion**

831   In this study, we examine the degree to which CONUS scale atmospheric deposition patterns,

832   vegetation trends, and stream trends can be potential indicators of watershed N-saturation,

833   retention, and recovery conditions, and how watershed N retention and losses vary over space

834   and time. We provide evidence for the hysteresis behavior of N-saturation and retention in

835   watersheds using a time series of CONUS stream losses relative to CONUS atmospheric

836   deposition inputs and NDVI. We highlight watershed N-retention patterns across groups of

837   atmospheric deposition and vegetation productivity/biomass to advance understanding of stream

838   trends as indicators of watershed N conditions, and reveal patterns of watershed N-hysteresis

839   (recovery) or transition patterns.

840

841   **4.1 Stream Trends Reveal Watershed N-Hysteresis Patterns**

842

843   Several lines of evidence here support the hysteretic conceptual model of watershed N

844   retention and recovery (Figure 2). First, we found that atmospheric deposition (TDEP) and

845   vegetation (NDVI) groups that display combinations of strong positive or negative trends over

846   time, are associated with patterns of stream exports that uniquely indicate the stage of watershed

847   N-saturation (Figure 8) and reveal modalities of watershed N-retention hysteresis or one-way

848   transition patterns (Figure 11). In particular, we found regions with increasing TDEP and

849   increasing NDVI *trends* (Group a, Figure 2) have close to 100% N-retention (Figure 9c), become

850   increasingly N-saturated over time (Figure 11) and are associated with the strongest declines in

851   DIN and DOC exports (Figure 8). Conversely, we find a tendency towards increasing trends in

852   DIN exports and much lower retention in regions associated with TDEP-NDVI Group d where

853   watersheds retain about 50 - 66 % of incoming TDEP. Second, trends in DIN export that

854   coincide with trends in DOC export also help to identify the stage of watershed N-retention and

855   direction of change based on our updated N-hysteresis conceptual model. Since DOC movement

856   to streams is a function of the size of the watershed C pool, in-stream DOC concentration

857   measurements combined with DIN measurements can provide an important proxy of catchment

858   responses to N deposition and input. Third, by examining how watershed N-retention has

859   changed over time, we found that watersheds display a variety of types of recovery (hysteresis)

860   or non-recovery (one-way) patterns. Our findings agree with the hypotheses presented by Lovett

861   et al., (2018) that areas at late successional stages (i.e., those in Group d) should show much less

862   retention than their aggrading counterparts (Group a). We hope that our work can provide value

863   to future interpretation of in-stream trends and provides a new conceptual model such that in-

864   stream DIN and DOC *trend* signatures can be used as indicators of watershed N-retention status

865   (Gilliam et al., 2019; Goodale et al., 2003, 2005).

866

867   **4.2 Drivers of N-retention, and hysteresis patterns across the CONUS**

868   We found that regional trends in-stream exports (*Ex*) were more often correlated to trends in

869   concentration (*Cn*) rather than trends in discharge (*Qs*). This reveals that the dominant

870   contributing factor to *changes in magnitude and direction of trends* of *Ex* are more often

871   determined by changes in concentrations than flow. This emphasizes the significant role of 1)

872   watershed biogeochemical cycling and processes (soil and biomass immobilization, in-stream

873   biogeochemistry etc.) across the critical zone as major factors shaping in-stream concentrations,

874   and 2) the significant role of environmental physical/chemical conditions (TDEP-NDVI group)

875   that facilitate uptake and retention of N. While the lack of influence of *Qs* has been noted

876   previously (Goodale et al., 2003; Lucas et al., 2016), drivers of trends in *Ex* can be hydrological,

877   biogeochemical, or an external factor (e.g. agriculture), whereas, the observed trends in *Qs* and

878   *Cn* can be indicators of changing watershed N functionality through vegetative, soil, or in-stream

879   biogeochemical pathways. For example, the insignificant role of discharge trends on determining

880   overall trends in exports and concentrations may be more directly related to the stage of

881   watershed N-saturation, evapotranspiration control on depth of hydrological flow paths, and

882   newly acquired access of flowpaths to stores of older N and C not readily assessable prior to

883   transitions in TDEP-NDVI stage (Barnes et al., 2018). Indeed, residence times of water versus N

884   particles within a watershed are different and can vary from years to decades depending on inter-

885   annual or anthropogenic conditions (Sinha & Michalak, 2016). Much recent work in watershed

886   acid-rain mitigation experiments suggests that the 'flashiness' of N export during storm events

887   might be an important indicator of watershed N-retention and saturation status because of shifts

888   in N sourcing form more distal and shallow parts of the watershed (Marinos et al., 2018). Despite

889   the lack of significant trends in discharge observed in our study, more work will be needed

890   assessing how hydrological conditions coincide with broad scale physical/chemical conditions as

891   described by TDEP-NDVI patterns that impact flow paths and access to different stores and

892   cycling of C and N in landscapes.

893

894   **4.3 In-stream processes**

895   The second-largest factor explaining variability in watershed N-retention across HUC2

896   basins was in-stream temperature and DOC concentration trends (Table 3). This result provides

897   evidence that in-stream measurements can potentially can be indicators of watershed

898   functionality by interpreting stream signals as aggregated measurements and proxies to those

899   upstream watershed conditions. The consequence of changing N and C transfer from the

900   terrestrial to the aquatic setting is the mediation of in-stream assimilation and hyporheic redox

901   conditions at downstream locations. In-stream and hyporheic biogeochemistry provides an

902   important control on stream exports once nutrients reach the stream through in-stream

903   assimilation and hyporheic denitrification (Arora et al., 2016; Cejudo et al., 2018; Hood et al.,

904   2017). Declining stream N exports due to increased watershed N retention may lead to steady or

905   increasing DO concentrations in downstream ecosystems and transition to oligotrophic

906   conditions (Craine et al., 2018; Groffman et al., 2018). Changes in aquatic primary production

907   can occur in response to changing nitrogen inputs (from atmospheric deposition and watershed

908   delivery) and seasonality (Bernhardt & Likens, 2004), which can shift denitrification rates and

909   patterns through direct and indirect coupling to labile carbon exudates and oxygen conditions

910   (Heffernan & Cohen, 2010). Conversely, in low elevation or more anthropogenic sites, rising

911   temperatures and increases in N transfer to streams could coincide with declining DO

912   concentrations and more eutrophic conditions, greater in-stream N-assimilation, particularly in

913   N-limited water bodies (Beaulieu et al., 2011; Bernhardt et al., 2002; Halliday et al., 2013), and

914   greater hyporheic denitrification (Bernhardt et al., 2005; Duncan et al., 2013, 2015; Maavara et

915   al., 2019; Mulholland et al., 2009; Newcomer et al., 2018; Seitzinger et al., 2006). The influence

916   of stream factors on watershed N-retention before land use/cover was a surprising aspect of this

917   analysis. Because stream and hyporheic residence times are so short, this conclusion indicates

918   that instream processes are probably substantially more influential than expected, in terms of the

919   overall magnitude of control on stream exports.

920

921   **4.4 Confounding factors**

922   We found that watershed retention is quite high (>70% for most watersheds across the U.S.)

923   relative to atmospheric inputs, a finding similar to other published work (Lovett et al., 2000). It is

924   important to note that any external contributions to in-stream DIN concentrations and exports not

925   accounted for in this study (i.e. agriculture) would be additional input terms in the retention

926   equation. These retention estimates are likely an underestimate of watershed N retention because

927   there is uncertainty related to source terms from the lack of information on anthropogenic inputs

928   across these watersheds. We do not account for agriculture input to our retention equation which

929   means that our retention estimates are potentially significant *underestimates* of retention. Since

930   exports and TDEP are the measured values in the retention equation, we estimate that in the most

931   intensively managed agricultural regions, we are underestimating retention by 50-100% (25

932   Kg/hectare/year)(Van Meter et al., 2016).

933   Surprisingly, while we found that land cover, and in particular land cover change data

934   was the least significant factor controlling N export and retention, we acknowledge that

935   consideration of potential drivers of some stream N trends depends somewhat on to what extent

936   these watersheds receive urban or agricultural N inputs and how these have changed. For

937   example, we found more spatially consistent decreasing trends in stream DAA exports and

938   concentrations across the CONUS which might be more likely to reflect change in fertilizer or

939   sewage N inputs. The lack of significance between watershed N-retention and land cover/change

940   data may also point to legacy N in watersheds. Given the history of N deposition and

941   anthropogenic application on ecosystems, there is great potential for lagged responses and

942   geochemical stationarity in stream N and C because of significant water and N residence times

943   (Basu et al., 2010).

944   Other confounding factors not included in this analysis are the occurrence of extreme event

945   hydrological conditions (Argerich et al., 2013), shifts in the abundance of dominant vegetation

946   within classes (Argerich et al., 2013; Bernal et al., 2012; Compton et al., 2003; Rhoades et al.,

947   2017; Sudduth et al., 2013; Van Breemen et al., 2002), changes in vegetation aboveground

948   biomass and plant populations in response to varying alpine snow-hydrological conditions

949   (Hubbard et al., 2018), and changes in reforested areas could explain an overall decline in NO_3^-

950   export within the stream (Bernal et al., 2012). In other studies, declines of in-stream N have been

951   found in regions with greatest soil N accumulation and during the growing season indicating a

952   biologically mediated trend in DIN and no correlation with hydrology (Lucas et al., 2016).

953   Similar to Goodale et al., (2005) we find patterns in DOC concentrations across these watersheds

954   that support the hypothesized mechanism that enhanced ecosystem productivity increases fluxes

955   of labile carbon from the soil to the stream, enhancing denitrification leading to declining stream

956   N trends. Finally, the importance of climatic control on soil N processes cannot be emphasized

957   enough. Longer growing seasons, with warmer climates and elevated CO_2 have been shown to

958   change nitrogen and carbon availability terrestrial soils (Terrer et al., 2018). Plant uptake and N

959   mineralization both respond to soil moisture, temperature, and climatic patterns such that any

960   changes in the rate or timing of these processes can tilt watersheds beyond their ability to retain

961   or release nitrogen in a hysteretic manner.

962

963

964   **5.0 Conclusion**

965   In many watersheds across the CONUS, stream exports of DIN have been declining and

966   show enduring legacies from N-deposition and acid rain. To examine large scale controls on

967   stream DIN and DOC concentration and export trends, we developed an updated hysteresis

968   conceptual model of watershed N-retention and examined how two main controlling landscape-

969   scale controls (TDEP and NDVI) can be used to group patterns of stream loss and watershed

970   retention. Our hysteresis conceptual model provides a novel framework for which to assess

971   watershed N-retention and recovery patters as indicated by stream DIN and DOC trends. Our

972   conceptual model is validated with a quantitative analysis of stream data (DIN, DOC,

973   temperature), NDVI, land cover, and TDEP trends that reveal specific patterns of stream loss that

974   are associated with modalities of watershed hysteresis (recovery) or one-way transition (new

975   steady state) patterns. For the first time, we show that watershed retention of N can display

976   unique hysteresis patterns, and that these patterns can be explained by the wealth of detailed

977   mechanistic studies available for watersheds at different stages of response to changing N-

978   deposition. In its present form, our conceptual model can offer a valuable new insight into

979 decade's worth of stream water data collection, and highlight the value of stream water

980 measurements as critical indicators of upstream watershed functionality.

981
982 **6.0 Acknowledgements**

1002
1003   **7.0 Author Contributions**

1004   MN, HW, NB, SH contributed to experimental design. MN, DD, KW, and HW contributed to

1005   data collection and analysis. MN, DD, EW contributed to code design. MN, NB, TM, BA, EW,

1006   KW, CS, SH contributed to data interpretation. MN prepared the manuscript with contributions

1007   from all authors.

1008
1009   **8.0 References**

1010   Aber, J. D., McDowell, W., Nadelhoffer, K., Magill, A., Berntson, G., Kamakea, M., et al.

1011   (1998). Nitrogen Saturation in Temperate Forest Ecosystems. *BioScience*, *48*(11), 921–

1012   934. https://doi.org/10.2307/1313296

1013   Aber, J. D., Goodale, C. L., Ollinger, S. V., Smith, M.-L., Magill, A. H., Martin, M. E., et al.

1014   (2003). Is Nitrogen Deposition Altering the Nitrogen Status of Northeastern Forests?

1015   *BioScience*, *53*(4), 375. https://doi.org/10.1641/0006-

1016   3568(2003)053[0375:INDATN]2.0.CO;2

1017   Argerich, A., Johnson, S. L., Sebestyen, S. D., Rhoades, C. C., Greathouse, E., Knoepp, J. D., et

1018   al. (2013). Trends in stream nitrogen concentrations for forested reference catchments

1019   across the USA. *Environmental Research Letters*, *8*(1), 014039.

1020   https://doi.org/10.1088/1748-9326/8/1/014039

1021   Arora, B., Spycher, N. F., Steefel, C. I., Molins, S., Bill, M., Conrad, M. E., et al. (2016).

1022   Influence of hydrological, biogeochemical and temperature transients on subsurface

1023   carbon fluxes in a flood plain environment. *Biogeochemistry*, *127*(2–3), 367–396.

1024   https://doi.org/10.1007/s10533-016-0186-8

1025   Ballard, T. C., Sinha, E., & Michalak, A. M. (2019). Long-Term Changes in Precipitation and

1026   Temperature Have Already Impacted Nitrogen Loading. *Environmental Science &*

1027   *Technology*, *53*(9), 5080–5090. https://doi.org/10.1021/acs.est.8b06898

1028   Barnes, R. T., Butman, D. E., Wilson, H. F., & Raymond, P. A. (2018). Riverine Export of Aged

1029   Carbon Driven by Flow Path Depth and Residence Time. *Environmental Science &*

1030   *Technology*, *52*(3), 1028–1035. https://doi.org/10.1021/acs.est.7b04717

1031   Beaulieu, J. J., Tank, J. L., Hamilton, S. K., Wollheim, W. M., Hall, R. O., Mulholland, P. J., et

1032   al. (2011). Nitrous oxide emission from denitrification in stream and river networks.

1033   *Proceedings of the National Academy of Sciences*, *108*(1), 214–219.

1034   https://doi.org/10.1073/pnas.1011464108

1035   Bellmore, R. A., Compton, J. E., Brooks, J. R., Fox, E. W., Hill, R. A., Sobota, D. J., et al.

1036   (2018). Nitrogen inputs drive nitrogen concentrations in U.S. streams and rivers during

1037   summer low flow conditions. *Science of The Total Environment*, *639*, 1349–1359.

1038   https://doi.org/10.1016/j.scitotenv.2018.05.008

1039   Bernal, S., Hedin, L. O., Likens, G. E., Gerber, S., & Buso, D. C. (2012). Complex response of

1040   the forest nitrogen cycle to climate change. *Proceedings of the National Academy of*

1041   *Sciences*, *109*(9), 3406–3411. https://doi.org/10.1073/pnas.1121448109

1042   Bernhardt, E. S., & Likens, G. E. (2004). Controls on periphyton biomass in heterotrophic

1043   streams. *Freshwater Biology*, *49*(1), 14–27. https://doi.org/10.1046/j.1365-

1044   2426.2003.01161.x

1045   Bernhardt, E. S., Hall, Jr., R. O., & Likens, G. E. (2002). Whole-system Estimates of

1046   Nitrification and Nitrate Uptake in Streams of the Hubbard Brook Experimental Forest.

1047   *Ecosystems*, *5*(5), 419–430. https://doi.org/10.1007/s10021-002-0179-4

1048   Bernhardt, E. S., Likens, G. E., Hall, R. O., Buso, D. C., Fisher, S. G., Burton, T. M., et al.

1049   (2005). Can't See the Forest for the Stream? In-stream Processing and Terrestrial

1050   Nitrogen Exports. *BioScience*, *55*(3), 219. https://doi.org/10.1641/0006-

1051   3568(2005)055[0219:ACSTFF]2.0.CO;2

1052   Bowden, R. D., Wurzbacher, S. J., Washko, S. E., Wind, L., Rice, A. M., Coble, A. E., et al.

1053   (2019). Long-term Nitrogen Addition Decreases Organic Matter Decomposition and

1054   Increases Forest Soil Carbon. *Soil Science Society of America Journal*, *83*(S1).

1055   https://doi.org/10.2136/sssaj2018.08.0293

1056   Boyer, E. W., Howarth, R. W., Galloway, J. N., Dentener, F. J., Green, P. A., & Vörösmarty, C.

1057   J. (2006). Riverine nitrogen export from the continents to the coasts: RIVERINE

1058   NITROGEN EXPORT. *Global Biogeochemical Cycles*, *20*(1), n/a-n/a.

1059   https://doi.org/10.1029/2005GB002537

1060   Cejudo, E., Hood, J. L., Schiff, S. L., & Aravena, R. O. (2018). Using the $\delta15N$ of submerged

1061   biomass for assessing changes in the nitrogen cycling in a river receiving wastewater

1062   treated effluent. *Ecological Indicators*, *95*, 645–653.

1063   https://doi.org/10.1016/j.ecolind.2018.08.013

1064   Compton, J. E., Church, M. R., Larned, S. T., & Hogsett, W. E. (2003). Nitrogen Export from

1065   Forested Watersheds in the Oregon Coast Range: The Role of N 2 -fixing Red Alder.

1066   *Ecosystems*, *6*(8), 773–785. https://doi.org/10.1007/s10021-002-0207-4

1067   Craine, J. M., Elmore, A. J., Wang, L., Aranibar, J., Bauters, M., Boeckx, P., et al. (2018).

1068   Isotopic evidence for oligotrophication of terrestrial ecosystems. *Nature Ecology &*

1069   *Evolution*, *2*(11), 1735–1744. https://doi.org/10.1038/s41559-018-0694-0

1070   Crawford, J. T., Hinckley, E.-L. S., Litaor, M. I., Brahney, J., & Neff, J. C. (2019). Evidence for

1071   accelerated weathering and sulfate export in high alpine environments. *Environmental*

1072   *Research Letters*, *14*(12), 124092. https://doi.org/10.1088/1748-9326/ab5d9c

1073   Cusack, D. F., Silver, W. L., Torn, M. S., Burton, S. D., & Firestone, M. K. (2011). Changes in

1074   microbial community characteristics and soil organic matter with nitrogen additions in

1075   two tropical forests. *Ecology*, *92*(3), 621–632. https://doi.org/10.1890/10-0459.1

1076   Driscoll, C. T., Driscoll, K. M., Roy, K. M., & Mitchell, M. J. (2003). Chemical Response of

1077   Lakes in the Adirondack Region of New York to Declines in Acidic Deposition.

1078   *Environmental Science & Technology*, *37*(10), 2036–2042.

1079   https://doi.org/10.1021/es020924h

1080   Duncan, J. M., Groffman, P. M., & Band, L. E. (2013). Towards closing the watershed nitrogen

1081   budget: Spatial and temporal scaling of denitrification. *Journal of Geophysical Research:*

1082   *Biogeosciences*, *118*(3), 1105–1119. https://doi.org/10.1002/jgrg.20090

1083   Duncan, J. M., Band, L. E., Groffman, P. M., & Bernhardt, E. S. (2015). Mechanisms driving the

1084   seasonality of catchment scale nitrate export: Evidence for riparian ecohydrologic

1085   controls: SEASONALITY OF CATCHMENT NITRATE EXPORT. *Water Resources*

1086   *Research*, *51*(6), 3982–3997. https://doi.org/10.1002/2015WR016937

1087   Dwivedi, D., & Mohanty, B. (2016). Hot Spots and Persistence of Nitrate in Aquifers Across

1088   Scales. *Entropy*, *18*(1), 25. https://doi.org/10.3390/e18010025

1089   EPA CASTNET. (2019). Clean Air Status and Trends Network (CASTNET) EPA CASTNET

1090   Total Wet and Dry Deposition. Retrieved from https://www.epa.gov/castnet

1091   Eshleman, K. N., Sabo, R. D., & Kline, K. M. (2013). Surface Water Quality Is Improving due to

1092   Declining Atmospheric N Deposition. *Environmental Science & Technology*, *47*(21),

1093   12193–12200. https://doi.org/10.1021/es4028748

1094   Evans, C. D., Reynolds, B., Jenkins, A., Helliwell, R. C., Curtis, C. J., Goodale, C. L., et al.

1095   (2006). Evidence that Soil Carbon Pool Determines Susceptibility of Semi-Natural

1096   Ecosystems to Elevated Nitrogen Leaching. *Ecosystems*, *9*(3), 453–462.

1097   https://doi.org/10.1007/s10021-006-0051-z

1098   Forbes, W. L., Mao, J., Ricciuto, D. M., Kao, S., Shi, X., Tavakoly, A. A., et al. (2019).

1099   Streamflow in the Columbia River Basin: Quantifying Changes Over the Period 1951-

1100   2008 and Determining the Drivers of Those Changes. *Water Resources Research*, *55*(8),

1101   6640–6652. https://doi.org/10.1029/2018WR024256

1102   Garayburu-Caruso, V. A., Stegen, J. C., Song, H.-S., Renteria, L., Wells, J., Garcia, W., et al.

1103   (2020). Carbon Limitation Leads to Thermodynamic Regulation of Aerobic Metabolism.

1104   *Environmental Science & Technology Letters*, acs.estlett.0c00258.

1105   https://doi.org/10.1021/acs.estlett.0c00258

1106   Gilliam, F. S., Burns, D. A., Driscoll, C. T., Frey, S. D., Lovett, G. M., & Watmough, S. A.

1107   (2019). Decreased atmospheric nitrogen deposition in eastern North America: Predicted

1108   responses of forest ecosystems. *Environmental Pollution*, *244*, 560–574.

1109   https://doi.org/10.1016/j.envpol.2018.09.135

1110   Goodale, C. L., Aber, J. D., & Vitousek, P. M. (2003). An Unexpected Nitrate Decline in New

1111   Hampshire Streams. *Ecosystems*, *6*(1), 0075–0086. https://doi.org/10.1007/s10021-002-

1112   0219-0

1113   Goodale, C. L., Aber, J. D., Vitousek, P. M., & McDowell, W. H. (2005). Long-term Decreases

1114   in Stream Nitrate: Successional Causes Unlikely; Possible Links to DOC? *Ecosystems*,

1115   *8*(3), 334–337. https://doi.org/10.1007/s10021-003-0162-8

1116   Groffman, P. M., Driscoll, C. T., Durán, J., Campbell, J. L., Christenson, L. M., Fahey, T. J., et

1117   al. (2018). Nitrogen oligotrophication in northern hardwood forests. *Biogeochemistry*,

1118   *141*(3), 523–539. https://doi.org/10.1007/s10533-018-0445-y

1119   Guo, D., Lintern, A., Webb, J. A., Ryu, D., Liu, S., Bende-Michl, U., et al. (2019). Key Factors

1120   Affecting Temporal Variability in Stream Water Quality. *Water Resources Research*,

1121   *55*(1), 112–129. https://doi.org/10.1029/2018WR023370

1122   Hale, R. L., Grimm, N. B., Vörösmarty, C. J., & Fekete, B. (2015). Nitrogen and phosphorus

1123   fluxes from watersheds of the northeast U.S. from 1930 to 2000: Role of anthropogenic

1124   nutrient inputs, infrastructure, and runoff. *Global Biogeochemical Cycles*, *29*(3), 341–

1125   356. https://doi.org/10.1002/2014GB004909

1126   Halliday, S. J., Skeffington, R. A., Wade, A. J., Neal, C., Reynolds, B., Norris, D., & Kirchner, J.

1127   W. (2013). Upland streamwater nitrate dynamics across decadal to sub-daily timescales:

1128   a case study of Plynlimon, Wales. *Biogeosciences*, *10*(12), 8013–8038.

1129   https://doi.org/10.5194/bg-10-8013-2013

1130   Heffernan, J. B., & Cohen, M. J. (2010). Direct and indirect coupling of primary production and

1131   diel nitrate dynamics in a subtropical spring-fed river. *Limnology and Oceanography*,

1132   *55*(2), 677–688. https://doi.org/10.4319/lo.2010.55.2.0677

1133   Helsel, D. R., & Hirsch, R. M. (2002). *Statistical Methods in Water Resources*. U.S. Geological

1134   Survey. Retrieved from http://pubs.usgs.gov/twri/twri4a3/

1135   Hirsch, R. M., & De Cicco, L. (2015). *User guide to Exploration and Graphics for RivEr Trends*

1136   *(EGRET) and dataRetrieval: R packages for hydrologic data (version 2.0, February*

1137   *2015)*. Retrieved from https://dx.doi.org/10.3133/tm4A10

1138   Hirsch, R. M., Moyer, D. L., & Archfield, S. A. (2010). Weighted Regressions on Time,

1139   Discharge, and Season (WRTDS), with an Application to Chesapeake Bay River Inputs.

1140   *JAWRA Journal of the American Water Resources Association*, *46*(5), 857–880.

1141   https://doi.org/10.1111/j.1752-1688.2010.00482.x

1142   Hood, J. M., Benstead, J. P., Cross, W. F., Huryn, A. D., Johnson, P. W., Gíslason, G. M., et al.

1143   (2017). Increased resource use efficiency amplifies positive response of aquatic primary

1144   production to experimental warming. *Global Change Biology*.

1145   https://doi.org/10.1111/gcb.13912

1146   Hubbard, S. S., Williams, K. H., Agarwal, D., Banfield, J., Beller, H., Bouskill, N., et al. (2018).

1147   The East River, Colorado, Watershed: A Mountainous Community Testbed for

1148   Improving Predictive Understanding of Multiscale Hydrological–Biogeochemical

1149   Dynamics. *Vadose Zone Journal*, *17*(1), 0. https://doi.org/10.2136/vzj2018.03.0061

1150   Hungate, B. A., Lund, C. P., Pearson, H. L., & Chapin, Iii, F. S. (1997). Elevated CO2 and

1151   nutrient addition after soil N cycling and N trace gas fluxes with early season wet-up in a

1152   California annual grassland. *Biogeochemistry*, *37*(2), 89–109.

1153   https://doi.org/10.1023/A:1005747123463

1154   Huntington, T. G. (2005). Can Nitrogen Sequestration Explain the Unexpected Nitrate Decline in

1155   New Hampshire Streams? *Ecosystems*, *8*(3), 331–333. https://doi.org/10.1007/s10021-

1156   004-0105-z

1157   Hurst, H. E. (1951). Long-term Storage Capacity of Resevoirs. In *Transactions of the American*

1158   *Society of Civil Engineers* (Vol. 116, pp. 770–799). American Society of Civil Engineers.

1159   Janssens, I. A., Dieleman, W., Luyssaert, S., Subke, J.-A., Reichstein, M., Ceulemans, R., et al.

1160   (2010). Reduction of forest soil respiration in response to nitrogen deposition. *Nature*

1161   *Geoscience*, *3*(5), 315–322. https://doi.org/10.1038/ngeo844

1162   Jensen, A. M., Scanlon, T. M., & Riscassi, A. L. (2017). Emerging investigator series: the effect

1163   of wildfire on streamwater mercury and organic carbon in a forested watershed in the

1164   southeastern United States. *Environmental Science: Processes & Impacts*, *19*(12), 1505–

1165   1517. https://doi.org/10.1039/C7EM00419B

1166   Kothawala, D. N., Watmough, S. A., Futter, M. N., Zhang, L., & Dillon, P. J. (2011). Stream

1167   Nitrate Responds Rapidly to Decreasing Nitrate Deposition. *Ecosystems*, *14*(2), 274–286.

1168   https://doi.org/10.1007/s10021-011-9422-1

1169   Lawrence, G. B., Scanga, S. E., & Sabo, R. D. (2020). Recovery of Soils From Acidic

1170   Deposition May Exacerbate Nitrogen Export From Forested Watersheds. *Journal of*

1171   *Geophysical Research: Biogeosciences*, *125*(1). https://doi.org/10.1029/2019JG005036

1172   Li, Y., Schichtel, B. A., Walker, J. T., Schwede, D. B., Chen, X., Lehmann, C. M. B., et al.

1173   (2016). Increasing importance of deposition of reduced nitrogen in the United States.

1174   *Proceedings of the National Academy of Sciences*, *113*(21), 5874–5879.

1175   https://doi.org/10.1073/pnas.1525736113

1176   Lovett, G. M., & Goodale, C. L. (2011). A New Conceptual Model of Nitrogen Saturation Based

1177   on Experimental Nitrogen Addition to an Oak Forest. *Ecosystems*, *14*(4), 615–631.

1178   https://doi.org/10.1007/s10021-011-9432-z

1179   Lovett, G. M., Weathers, K. C., & Sobczak, W. V. (2000). Nitrogen Saturation and Retention in

1180   the Forested Watersheds of the Catskill Mountains, New York. *Ecological Applications*,

1181   *10*(1), 73–84. https://doi.org/10.1890/1051-0761(2000)010[0073:NSARIF]2.0.CO;2

1182   Lovett, G. M., Goodale, C. L., Ollinger, S. V., Fuss, C. B., Ouimette, A. P., & Likens, G. E.

1183   (2018). Nutrient retention during ecosystem succession: a revised conceptual model.

1184   *Frontiers in Ecology and the Environment*, *16*(9), 532–538.

1185   https://doi.org/10.1002/fee.1949

1186   Lucas, R. W., Klaminder, J., Futter, M. N., Bishop, K. H., Egnell, G., Laudon, H., & Högberg, P.

1187   (2011). A meta-analysis of the effects of nitrogen additions on base cations: Implications

1188   for plants, soils, and streams. *Forest Ecology and Management*, *262*(2), 95–104.

1189   https://doi.org/10.1016/j.foreco.2011.03.018

1190   Lucas, R. W., Sponseller, R. A., Gundale, M. J., Stendahl, J., Fridman, J., Högberg, P., &

1191   Laudon, H. (2016). Long-term declines in stream and river inorganic nitrogen (N) export

1192   correspond to forest change. *Ecological Applications*, *26*(2), 545–556.

1193   https://doi.org/10.1890/14-2413

1194   Maavara, T., Lauerwald, R., Laruelle, G. G., Akbarzadeh, Z., Bouskill, N. J., Van Cappellen, P.,

1195   & Regnier, P. (2019). Nitrous oxide emissions from inland waters: Are IPCC estimates

1196   too high? *Global Change Biology*, *25*(2), 473–488. https://doi.org/10.1111/gcb.14504

1197   Marinos, R. E., Campbell, J. L., Driscoll, C. T., Likens, G. E., McDowell, W. H., Rosi, E. J., et

1198   al. (2018). Give and Take: A Watershed Acid Rain Mitigation Experiment Increases

1199   Baseflow Nitrogen Retention but Increases Stormflow Nitrogen Export. *Environmental*

1200   *Science & Technology*, *52*(22), 13155–13165. https://doi.org/10.1021/acs.est.8b03553

1201   Maurer, E. P. (2016). CONUS digital elevation model of 1/16 degree grid cells. Retrieved from

1202   https://www.hydroshare.org/resource/c18cef883695498c81acf9c4260d1e53/

1203   Maurer, E. P., Lettenmaier, D. P., & Mantua, N. J. (2004). Variability and potential sources of

1204   predictability of North American runoff. *Water Resources Research*, *40*(9).

1205   https://doi.org/10.1029/2003WR002789

1206   Moatar, F., Abbott, B. W., Minaudo, C., Curie, F., & Pinay, G. (2017). Elemental properties,

1207   hydrology, and biology interact to shape concentration-discharge curves for carbon,

1208   nutrients, sediment, and major ions: SHAPES AND CAUSES OF C-Q

1209   RELATIONSHIPS. *Water Resources Research*, *53*(2), 1270–1287.

1210   https://doi.org/10.1002/2016WR019635

1211   Monteith, D. T., Stoddard, J. L., Evans, C. D., de Wit, H. A., Forsius, M., Høgåsen, T., et al.

1212   (2007). Dissolved organic carbon trends resulting from changes in atmospheric

1213   deposition chemistry. *Nature*, *450*(7169), 537–540. https://doi.org/10.1038/nature06316

1214   Moritz, S., Sardá, A., Bartz-Beielstein, T., Zaefferer, M., & Stork, J. (2015). Comparison of

1215   different Methods for Univariate Time Series Imputation in R. *ArXiv:1510.03924 [Cs,

1216   Stat]*. Retrieved from http://arxiv.org/abs/1510.03924

1217   MRLC NLCD. (2020). NLCD Land Cover Change Index (CONUS) Multi-Resolution Land

1218   Characteristics (MRLC) consortium National Land Cover Database. Land Cover Change

1219   Index. Retrieved from https://www.mrlc.gov/data/nlcd-land-cover-change-index-conus

1220   Mulholland, P. J., Hall, R. O., Sobota, D. J., Dodds, W. K., Findlay, S. E. G., Grimm, N. B., et

1221   al. (2009). Nitrate removal in stream ecosystems measured by 15N addition experiments:

1222   Denitrification. *Limnology and Oceanography*, *54*(3), 666–680.

1223   https://doi.org/10.4319/lo.2009.54.3.0666

1224   Murphy, J., & Sprague, L. (2019). Water-quality trends in US rivers: Exploring effects from

1225   streamflow trends and changes in watershed management. *Science of The Total*

1226   *Environment*, *656*, 645–658. https://doi.org/10.1016/j.scitotenv.2018.11.255

1227   Murphy, S. F., Writer, J. H., McCleskey, R. B., & Martin, D. A. (2015). The role of precipitation

1228   type, intensity, and spatial distribution in source water quality after wildfire.

1229   *Environmental Research Letters*, *10*(8), 084007. https://doi.org/10.1088/1748-

1230   9326/10/8/084007

1231   Musolff, A., Schmidt, C., Selle, B., & Fleckenstein, J. H. (2015). Catchment controls on solute

1232   export. *Advances in Water Resources*, *86*, 133–146.

1233   https://doi.org/10.1016/j.advwatres.2015.09.026

1234   Musolff, A., Schmidt, C., Rode, M., Lischeid, G., Weise, S. M., & Fleckenstein, J. H. (2016).

1235   Groundwater head controls nitrate export from an agricultural lowland catchment.

1236   *Advances in Water Resources*, *96*, 95–107.

1237   https://doi.org/10.1016/j.advwatres.2016.07.003

1238   Musolff, A., Selle, B., Büttner, O., Opitz, M., & Tittel, J. (2017). Unexpected release of

1239   phosphate and organic carbon to streams linked to declining nitrogen depositions. *Global*

1240   *Change Biology*, *23*(5), 1891–1901. https://doi.org/10.1111/gcb.13498

1241   NADP. (2018). National Atmospheric Deposition Program (NRSP-3). NADP Program Office,

1242   Wisconsin State Laboratory of Hygiene, 465 Henry Mall, Madison, WI 53706. Retrieved

1243   October 24, 2018, from http://nadp.slh.wisc.edu/committees/tdep/tdepmaps/

1244   Newcomer, M. E., Hubbard, S. S., Fleckenstein, J. H., Maier, U., Schmidt, C., Thullner, M., et

1245   al. (2018). Influence of Hydrological Perturbations and Riverbed Sediment

1246   Characteristics on Hyporheic Zone Respiration of CO $_2$ and N $_2$. *Journal of Geophysical*

1247   *Research: Biogeosciences*, *123*(3), 902–922. https://doi.org/10.1002/2017JG004090

1248 O'Donnell, J. A., Aiken, G. R., Kane, E. S., & Jones, J. B. (2010). Source water controls on the

1249   character and origin of dissolved organic matter in streams of the Yukon River basin,

1250   Alaska. *Journal of Geophysical Research*, *115*(G3).

1251   https://doi.org/10.1029/2009JG001153

1252 Oelsner, G. P., & Stets, E. G. (2019). Recent trends in nutrient and sediment loading to coastal

1253   areas of the conterminous U.S.: Insights and global context. *Science of The Total*

1254   *Environment*, *654*, 1225–1240. https://doi.org/10.1016/j.scitotenv.2018.10.437

1255 Oelsner, G. P., Sprague, L. A., Murphy, J. C., Zuellig, R. E., Johnson, H. M., Ryberg, K. R., et

1256   al. (2017). *Water-quality trends in the Nation's rivers and streams, 1972–2012—Data*

1257   *preparation, statistical methods, and trend results (ver. 2.0, October 2017)* (Scientific

1258   Investigations Report No. U.S. Geological Survey Scientific Investigations Report 2017–

1259   5006) (p. 136). U.S. Geological Survey. Retrieved from

1260   https://doi.org/10.3133/sir20175006

1261 Pardo, L. H., Fenn, M. E., Goodale, C. L., Geiser, L. H., Driscoll, C. T., Allen, E. B., et al.

1262   (2011). Effects of nitrogen deposition and empirical nitrogen critical loads for ecoregions

1263   of the United States. *Ecological Applications*, *21*(8), 3049–3082.

1264   https://doi.org/10.1890/10-2341.1

1265 Pellerin, B. A., Bergamaschi, B. A., Gilliom, R. J., Crawford, C. G., Saraceno, J., Frederick, C.

1266   P., et al. (2014). Mississippi River Nitrate Loads from High Frequency Sensor

1267   Measurements and Regression-Based Load Estimation. *Environmental Science &*

1268   *Technology*, *48*(21), 12612–12619. https://doi.org/10.1021/es504029c

1269   Pinder, R. W., Davidson, E. A., Goodale, C. L., Greaver, T. L., Herrick, J. D., & Liu, L. (2012).

1270   Climate change impacts of US reactive nitrogen. *Proceedings of the National Academy of*

1271   *Sciences*, *109*(20), 7671–7675. https://doi.org/10.1073/pnas.1114243109

1272   Quilbé, R., Rousseau, A. N., Duchemin, M., Poulin, A., Gangbazo, G., & Villeneuve, J.-P.

1273   (2006). Selecting a calculation method to estimate sediment and nutrient loads in streams:

1274   Application to the Beaurivage River (Québec, Canada). *Journal of Hydrology*, *326*(1–4),

1275   295–310. https://doi.org/10.1016/j.jhydrol.2005.11.008

1276   R Core Team. (2014). R: A language and environment for statistical computing. Retrieved from

1277   http://www.R-project.org/.

1278   Read, E. K., Carr, L., De Cicco, L., Dugan, H. A., Hanson, P. C., Hart, J. A., et al. (2017). Water

1279   quality data for national-scale aquatic research: The Water Quality Portal. *Water*

1280   *Resources Research*, *53*(2), 1735–1745. https://doi.org/10.1002/2016WR019993

1281   Renwick, W. H., Vanni, M. J., Fisher, T. J., & Morris, E. L. (2018). Stream Nitrogen,

1282   Phosphorus, and Sediment Concentrations Show Contrasting Long-term Trends

1283   Associated with Agricultural Change. *Journal of Environmental Quality*, *47*(6), 1513–

1284   1521. https://doi.org/10.2134/jeq2018.04.0162

1285   Rhoades, C. C., Hubbard, R. M., & Elder, K. (2017). A Decade of Streamwater Nitrogen and

1286   Forest Dynamics after a Mountain Pine Beetle Outbreak at the Fraser Experimental

1287   Forest, Colorado. *Ecosystems*, *20*(2), 380–392. https://doi.org/10.1007/s10021-016-0027-

1288   6

1289   Rhoades, C. C., Chow, A. T., Covino, T. P., Fegel, T. S., Pierson, D. N., & Rhea, A. E. (2018).

1290   The Legacy of a Severe Wildfire on Stream Nitrogen and Carbon in Headwater

1291   Catchments. *Ecosystems*. https://doi.org/10.1007/s10021-018-0293-6

1292 SanClements, M. D., Fernandez, I. J., Lee, R. H., Roberti, J. A., Adams, M. B., Rue, G. A., &

1293   McKnight, D. M. (2018). Long-Term Experimental Acidification Drives Watershed

1294   Scale Shift in Dissolved Organic Matter Composition and Flux. *Environmental Science &*

1295   *Technology*, *52*(5), 2649–2657. https://doi.org/10.1021/acs.est.7b04499

1296 Schwede, D. B., & Lear, G. G. (2014). A novel hybrid approach for estimating total deposition in

1297   the United States. *Atmospheric Environment*, *92*, 207–220.

1298   https://doi.org/10.1016/j.atmosenv.2014.04.008

1299 Seaber, P. R., Kapinos, F. P., & Knapp, G. L. (1987). *Hydrologic Unit Maps* (USGS Water

1300   Supply Paper No. Water-Supply Paper 2294) (p. 63). U.S. Geological Survey. Retrieved

1301   from https://water.usgs.gov/GIS/huc.html

1302 Seitzinger, S., Harrison, J. A., Böhlke, J. K., Bouwman, A. F., Lowrance, R., Peterson, B., et al.

1303   (2006). Denitrifcation Across Landscapes and Watersheds: A Synthesis. *Ecological*

1304   *Applications*, *16*(6), 2064–2090. https://doi.org/10.1890/1051-

1305   0761(2006)016[2064:DALAWA]2.0.CO;2

1306 Shoda, M. E., Sprague, L. A., Murphy, J. C., & Riskin, M. L. (2019). Water-quality trends in

1307   U.S. rivers, 2002 to 2012: Relations to levels of concern. *Science of The Total*

1308   *Environment*, *650*, 2314–2324. https://doi.org/10.1016/j.scitotenv.2018.09.377

1309 Shultz, M., Pellerin, B., Aiken, G., Martin, J., & Raymond, P. (2018). High Frequency Data

1310   Exposes Nonlinear Seasonal Controls on Dissolved Organic Matter in a Large

1311   Watershed. *Environmental Science & Technology*, *52*(10), 5644–5652.

1312   https://doi.org/10.1021/acs.est.7b04579

1313   Sinha, E., & Michalak, A. M. (2016). Precipitation Dominates Interannual Variability of

1314   Riverine Nitrogen Loading across the Continental United States. *Environmental Science*

1315   *& Technology*, *50*(23), 12874–12884. https://doi.org/10.1021/acs.est.6b04455

1316   Smith, R. A., Alexander, R. B., & Wolman, M. G. (1987). Water-Quality Trends in the Nation's

1317   Rivers. *Science*, *235*(4796), 1607–1615. https://doi.org/10.1126/science.235.4796.1607

1318   Spruce, J. P., Gasser, G. E., & Hargrove, W. W. (2016). MODIS NDVI Data, Smoothed and

1319   Gap-filled, for the Conterminous US: 2000-2015. ORNL Distributed Active Archive

1320   Center. https://doi.org/10.3334/ORNLDAAC/1299

1321   Stegen, J. C., Johnson, T., Fredrickson, J. K., Wilkins, M. J., Konopka, A. E., Nelson, W. C., et

1322   al. (2018). Influences of organic carbon speciation on hyporheic corridor

1323   biogeochemistry and microbial ecology. *Nature Communications*, *9*(1), 585.

1324   https://doi.org/10.1038/s41467-018-02922-9

1325   Stoddard, J. L. (1994). Long-Term Changes in Watershed Retention of Nitrogen: Its Causes and

1326   Aquatic Consequences. In L. A. Baker (Ed.), *Environmental Chemistry of Lakes and*

1327   *Reservoirs* (Vol. 237, pp. 223–284). Washington, DC: American Chemical Society.

1328   https://doi.org/10.1021/ba-1994-0237.ch008

1329   Stoddard, J. L., Jeffries, D. S., Lükewille, A., Clair, T. A., Dillon, P. J., Driscoll, C. T., et al.

1330   (1999). Regional trends in aquatic recovery from acidification in North America and

1331   Europe. *Nature*, *401*(6753), 575–578. https://doi.org/10.1038/44114

1332   Stoddard, J. L., Van Sickle, J., Herlihy, A. T., Brahney, J., Paulsen, S., Peck, D. V., et al. (2016).

1333   Continental-Scale Increase in Lake and Stream Phosphorus: Are Oligotrophic Systems

1334   Disappearing in the United States? *Environmental Science & Technology*, *50*(7), 3409–

1335   3415. https://doi.org/10.1021/acs.est.5b05950

1336   Sudduth, E. B., Perakis, S. S., & Bernhardt, E. S. (2013). Nitrate in watersheds: Straight from

1337   soils to streams. *Journal of Geophysical Research: Biogeosciences*, *118*(1), 291–302.

1338   https://doi.org/10.1002/jgrg.20030

1339   Terrer, C., Vicca, S., Stocker, B. D., Hungate, B. A., Phillips, R. P., Reich, P. B., et al. (2018).

1340   Ecosystem responses to elevated CO_2 governed by plant-soil interactions and the cost of

1341   nitrogen acquisition. *New Phytologist*, *217*(2), 507–522.

1342   https://doi.org/10.1111/nph.14872

1343   USGS. (2016). USGS NWIS Station Mapper. Retrieved from

1344   http://maps.waterdata.usgs.gov/mapper/index.html

1345   USGS. (2018). National Water Information System-Web Interface. Retrieved from

1346   https://waterdata.usgs.gov/nwis

1347   Van Breemen, N., Boyer, E. W., Goodale, C. L., Jaworski, N. A., Paustian, K., Seitzinger, S. P.,

1348   et al. (2002). Where Did All the Nitrogen Go? Fate of Nitrogen Inputs to Large

1349   Watersheds in the Northeastern U.S.A. *Biogeochemistry*, *57/58*, 267–293.

1350   Van Meter, K. J., & Basu, N. B. (2015). Catchment Legacies and Time Lags: A Parsimonious

1351   Watershed Model to Predict the Effects of Legacy Storage on Nitrogen Export. *PLOS*

1352   *ONE*, *10*(5), e0125971. https://doi.org/10.1371/journal.pone.0125971

1353   Van Meter, K. J., & Basu, N. B. (2017). Time lags in watershed-scale nutrient transport: an

1354   exploration of dominant controls. *Environmental Research Letters*, *12*(8), 084017.

1355   https://doi.org/10.1088/1748-9326/aa7bf4

1356   Van Meter, K. J., Basu, N. B., Veenstra, J. J., & Burras, C. L. (2016). The nitrogen legacy:

1357   emerging evidence of nitrogen accumulation in anthropogenic landscapes. *Environmental*

1358   *Research Letters*, *11*(3), 035014. https://doi.org/10.1088/1748-9326/11/3/035014

1359   Vitousek, P. M., & Reiners, W. A. (1975). Ecosystem Succession and Nutrient Retention: A

1360   Hypothesis. *BioScience*, *25*(6), 376–381. https://doi.org/10.2307/1297148

1361   Vuorenmaa, J., Augustaitis, A., Beudert, B., Bochenek, W., Clarke, N., de Wit, H. A., et al.

1362   (2018). Long-term changes (1990–2015) in the atmospheric deposition and runoff water

1363   chemistry of sulphate, inorganic nitrogen and acidity for forested catchments in Europe in

1364   relation to changes in emissions and hydrometeorological conditions. *Science of The*

1365   *Total Environment*, *625*, 1129–1145. https://doi.org/10.1016/j.scitotenv.2017.12.245

1366   Wasserstein, R. L., & Lazar, N. A. (2016). The ASA Statement on *p* -Values: Context, Process,

1367   and Purpose. *The American Statistician*, *70*(2), 129–133.

1368   https://doi.org/10.1080/00031305.2016.1154108

1369   Yanai, R. D., Vadeboncoeur, M. A., Hamburg, S. P., Arthur, M. A., Fuss, C. B., Groffman, P.

1370   M., et al. (2013). From Missing Source to Missing Sink: Long-Term Changes in the

1371   Nitrogen Budget of a Northern Hardwood Forest. *Environmental Science & Technology*,

1372   *47*(20), 11440–11448. https://doi.org/10.1021/es4025723

1373   Yang, L., Jin, S., Danielson, P., Homer, C., Gass, L., Bender, S. M., et al. (2018). A new

1374   generation of the United States National Land Cover Database: Requirements, research

1375   priorities, design, and implementation strategies. *ISPRS Journal of Photogrammetry and*

1376   *Remote Sensing*, *146*, 108–123. https://doi.org/10.1016/j.isprsjprs.2018.09.006

1377   Zarnetske, J. P., Bouda, M., Abbott, B. W., Saiers, J., & Raymond, P. A. (2018). Generality of

1378   Hydrologic Transport Limitation of Watershed Organic Carbon Flux Across Ecoregions

1379   of the United States. *Geophysical Research Letters*, *45*(21), 11,702-11,711.

1380   https://doi.org/10.1029/2018GL080005

1381

1382